Title: Pathogen effector recognition-dependent association of NRG1 with EDS1 and SAG101 in TNL receptor immunity

Xinhua Sun[1‖], Dmitry Lapin[1,5‖], Joanna M. Feehan[2‖], Sara C. Stolze[3], Katharina Kramer[3], Joram A. Dongus[1], Jakub Rzemieniewski[1,6], Servane Blanvillain-Baufumé[1], Anne Harzen[3], Jaqueline Bautor[1], Paul Derbyshire[2], Frank L. H. Menke[2], Iris Finkemeier[3,6], Hirofumi Nakagami[1,3], Jonathan D.G. Jones[2*], Jane E. Parker[1,4*]

1 – Department of Plant-Microbe Interactions, Max Planck Institute for Plant Breeding Research, Carl-von-Linne-Weg 10, 50829 Cologne, Germany

2 – The Sainsbury Laboratory, University of East Anglia, Norwich, United Kingdom

3 – Proteomics group, Max Planck Institute for Plant Breeding Research, Carl-von-Linne-Weg 10, 50829 Cologne, Germany

4 - Cologne-Düsseldorf Cluster of Excellence on Plant Sciences (CEPLAS), 40225 Düsseldorf, Germany

5 – Present address: Plant–Microbe Interactions, Department of Biology, Utrecht University, 3584 CH Utrecht, The Netherlands

6 – Present address: Department of Phytopathology, TUM School of Life Sciences Weihenstephan, Technical University of Munich, Freising 85354, Germany

7 – Present address: Institute of Biology and Biotechnology of Plants, University of Muenster, Schlossplatz 7, 48149 Muenster, Germany

‖ These authors contributed equally

* Corresponding authors

Abstract

Plants utilise intracellular nucleotide-binding, leucine-rich repeat (NLR) immune receptors to detect pathogen effectors and activate local and systemic defence. NRG1 and ADR1 "helper" NLRs (RNLs), cooperate with enhanced disease susceptibility 1 (EDS1), senescence-associated gene 101 (SAG101) and phytoalexin-deficient 4 (PAD4) lipase-like proteins to mediate signalling from TIR domain NLR receptors (TNLs). However, the mechanism of RNL/EDS1-family protein cooperation is poorly understood. Here, we provide genetic and molecular evidence for exclusive EDS1/SAG101/NRG1 and EDS1/PAD4/ADR1 co-functions in TNL immunity. Using immunoprecipitation and mass spectrometry, we show effector recognition-dependent association of NRG1 with EDS1 and SAG101, but not PAD4. An EDS1-SAG101 complex associates with NRG1, and EDS1-PAD4 associates with ADR1, only in an immune-activated state. NRG1 requires an intact nucleotide-binding P-loop motif, and EDS1 a functional EP domain and its partner SAG101, for induced association and immunity. Thus, two distinct modules (NRG1/EDS1/SAG101 and ADR1/EDS1/PAD4) are required to execute TNL receptor defence signalling.

Introduction

Plants and animals have evolved structurally and functionally related cell surface and intracellular receptors that detect pathogen-derived molecules and activate innate immune responses. In both kingdoms, pathogen recognition by intracellular nucleotide-binding/leucine-rich repeat (NLR) receptors restricts disease [1]. Whereas mammals tend to have few functional NLR receptors, many plants have expanded and diversified NLR gene repertoires, likely in response to evolutionary pressure from host-adapted pathogens and pests [1, 2]. Despite these different trajectories, plant and mammalian NLRs behave similarly as conformational switches for triggering defence and immune-related death pathways [3]. Plant NLRs directly bind pathogen strain-specific virulence factors (called effectors) or sense their modification of host immunity targets [4]. NLR-effector recognition leads to a process called effector-triggered immunity (ETI) which stops pathogen infection and is often accompanied by localized host cell death [5].

Increasing evidence in mammals and plants suggests NLR activation results from induced NLR oligomerization to form signalling-active scaffolds [6]. Plant NLR receptors are classified on the basis of their N-terminal signalling domain architectures: Toll/interleukin-1 receptor/resistance (TIR) NLRs (or TNLs) and coiled-coil (CC) NLRs (CNLs). The cryo-EM structure of a pathogen-activated CNL pentamer, *Arabidopsis* ZAR1, shows that five N-terminal domain protomers assemble a putative membrane-associated pore or channel which might represent a CC-mediated mechanism for activating defence signalling [7]. By contrast, structures of two pathogen-activated TNL receptor tetramers, *Arabidopsis* RPP1 and tobacco (*Nicotiana benthamiana*) Roq1, reveal that the four N-terminal TIR domains become reorganized to create a holoenzyme [8, 9]. Studies show that TIR-domains have NAD^+ hydrolysis activity which, for plant TNLs, is necessary to initiate an authentic host immune response [10, 11]. Hence, CNL- and TNL receptor early outputs appear to be different, though both are initiated by recognition-dependent oligomerization.

How NLR activation is transmitted to downstream pathways in ETI is more obscure, although CNLs and TNLs converge on qualitatively similar transcriptional programmes that drive local and systemic resistance [12, 13, 14]. NLRs also cooperate with cell surface pattern recognition receptor (PRR) systems mediating pattern-triggered immunity (PTI) to confer a fully effective immune response [15, 16]. Moreover, CNLs and TNLs rely on a network of signalling NLRs (generically referred to as helper NLRs) to promote immunity and host cell death [17, 18, 19]. Two related sub-families of helper NLRs, N requirement gene 1 (NRG1) [20, 21] and activated disease resistance 1 (ADR1) [22], are characterized by an N-terminal four-helix bundle domain with

homology to *Arabidopsis* resistance to powdery mildew 8 (RPW8) and plant, fungal and mammalian mixed lineage kinase cell death executors (MLKLs) that have HET-S/LOP-B (HeLo) domains [23, 24]. These helper NLRs are called CC_R-NLRs (or RNLs) [17]. In *Arabidopsis*, two functionally redundant *NRG1* paralogues (*NRG1.1* and *NRG1*.2) and three redundant *ADR1* paralogs (*ADR1*, *ADR1-L1* and *ADR1-L2*) contribute genetically to different extents to resistance and host cell death mediated by CNL and TNL receptors against a range of pathogens [12, 19, 25, 26]. Functionally relevant interactions have not been found so far that would link RNLs molecularly to sensor NLRs or downstream signalling pathways.

The enhanced disease susceptibility 1 (EDS1) family of three lipase-like proteins, EDS1, senescence-associated gene 101 (SAG101) and phytoalexin deficient 4 (PAD4), constitutes a major NLR immunity signalling node [27]. *EDS1* is essential for TNL dependent ETI across flowering plant species [26, 28, 29] and forms mutually exclusive, functional heterodimers with SAG101 or PAD4 [30]. Genetic and biochemical characterisation of EDS1-SAG101 and EDS1-PAD4 dimers shows they have distinct functions in immunity [26, 30, 31, 32]. EDS1-SAG101 appears to have coevolved with NRG1 group RNLs to signal specifically in TNL triggered ETI [26]. By contrast, EDS1-PAD4, like ADR1 group RNLs, regulate a basal immunity response which, in *Arabidopsis*, slows virulent pathogen infection [12, 22, 25, 28, 32, 33] and is utilized for ETI by TNL and CNL receptors [12, 19, 32]. A major role of *EDS1-PAD4* and *ADR1* RNLs in *Arabidopsis* basal immunity is to transcriptionally boost a genetically parallel salicylic acid (SA) phytohormone defence sector, which mediates local and systemic defences and is vulnerable to pathogen effector manipulation [28, 33, 34]. Recent studies revealed there is functional cooperation between EDS1-SAG101 and NRG1 RNLs in TNL ETI in *Arabidopsis* and *Nicotiana benthamiana*, consistent with their co-occurrence in angiosperm phylogenies [26, 29, 35]. Similarly, *Arabidopsis pad4* and *adr1*-family mutants phenocopy each other in various ETI and basal immunity responses [25, 26]. Several groups have proposed that EDS1-SAG101 co-functions with NRG1s, and EDS1-PAD4 with ADR1s, thus constituting two distinct immunity signalling nodes downstream of NLR activation [21, 25, 26].

Here we present a genetic and biochemical characterization of how *Arabidopsis* NRG1 and ADR1 RNLs co-function with EDS1 family members in NLR triggered immunity. We show in Arabidopsis that *EDS1-SAG101-NRG1*s and *EDS1-PAD4-ADR1*s operate genetically as non-interchangeable signalling nodes in ETI. By performing immunoprecipitation and mass spectrometry analyses of Arabidopsis stable transgenic lines, we detect induced specific NRG1 association with EDS1 and SAG101 proteins and ADR1 association with EDS1 and PAD4 after TNL activation. We find in *Arabidopsis* stable transgenic lines and in *N. benthamiana* reconstitution assays that PTI activation is insufficient for NRG1-induced

association with EDS1 and SAG101. We further discover that key functional elements of both the EDS1-SAG101 heterodimer and NRG1 are necessary to form a functional protein complex. Our data provide a first molecular insight to two functionally different RNL signalling nodes operating with specific EDS1-family members to execute defences downstream of NLR receptor activation.

Results

Distinct *PAD4-ADR1* and *SAG101-NRG1* modules operate in *Arabidopsis* TNL$^{RRS1\text{-}RPS4}$ immunity

We tested in *Arabidopsis* whether individual components of the proposed *EDS1-PAD4-ADR1*s and *EDS1-SAG101-NRG1*s immunity modules [25, 26] are genetically interchangeable. We reasoned that replacement of *ADR1* by *NRG1* group members, and reciprocally *PAD4* by *SAG101*, would reveal cross-utilization of components. Combinations of previously characterized *Arabidopsis EDS1* family mutants (*pad4*, *sag101*, and *pad4 sag101*) with *ADR1* (*adr1 adr1-L1 adr1-L2*, denoted *a3*) [22] or *NRG1* group (*nrg1.1* and *nrg1.2*; denoted *n2* [26]) mutants were generated in accession Col-0 (Col). This produced mutant groups I, II and III (Fig. 1a), with group III containing between-module combinations. Group I, II and III mutants were tested for TNL$^{RRS1\text{-}RPS4}$ mediated resistance to *Pst avrRps4* infection in leaves, measured against wild-type Col-0 (Col, resistant), an *rrs1a rrs1b* (*rrs1ab*) mutant defective specifically in TNL$^{RRS1\text{-}RPS4}$ ETI [36], as well as *eds1* and an *a3 n2* 'helperless' mutant which are both fully susceptible to *Pst avrRps4* [12, 19, 25, 26]. In *Pst avrRps4* growth assays, *pad4 a3* phenocopied the partial resistance of *pad4* and *a3* single mutants, and *sag101 n2* phenocopied *sag101* and *n2* full resistance (Fig. 1b, c). The cross-pathway *pad4 n2* and *sag101 a3* combinations in Group III were as susceptible as *eds1*, *pad4 sag101* and *a3 n2* mutants (Fig. 1b, c). We further tested group I, II and III mutants for host cell death responses to *Pf*0-1 delivering *avrRps4*, visually at 24 h post infiltration (hpi) (Supplementary Fig. 1a) and by quantitative electrolyte leakage assays over 6 - 24 hpi (Supplementary Fig. 1b). This produced the same phenotypic clustering of mutants as the *Pst avrRps4* resistance assays. Put together, these data show that there is exclusive cooperation between *PAD4* and *ADR1* RNLs in a single pathway leading to restriction of bacterial growth, and between *SAG101* and *NRG1* RNLs in promoting host cell death and resistance in TNL$^{RRS1\text{-}RPS4}$ immunity. Furthermore, the data argue strongly against physiologically relevant cross-utilization of components between the *PAD4-ADR1*s and *SAG101-NRG1*s signalling modules.

Figure 1

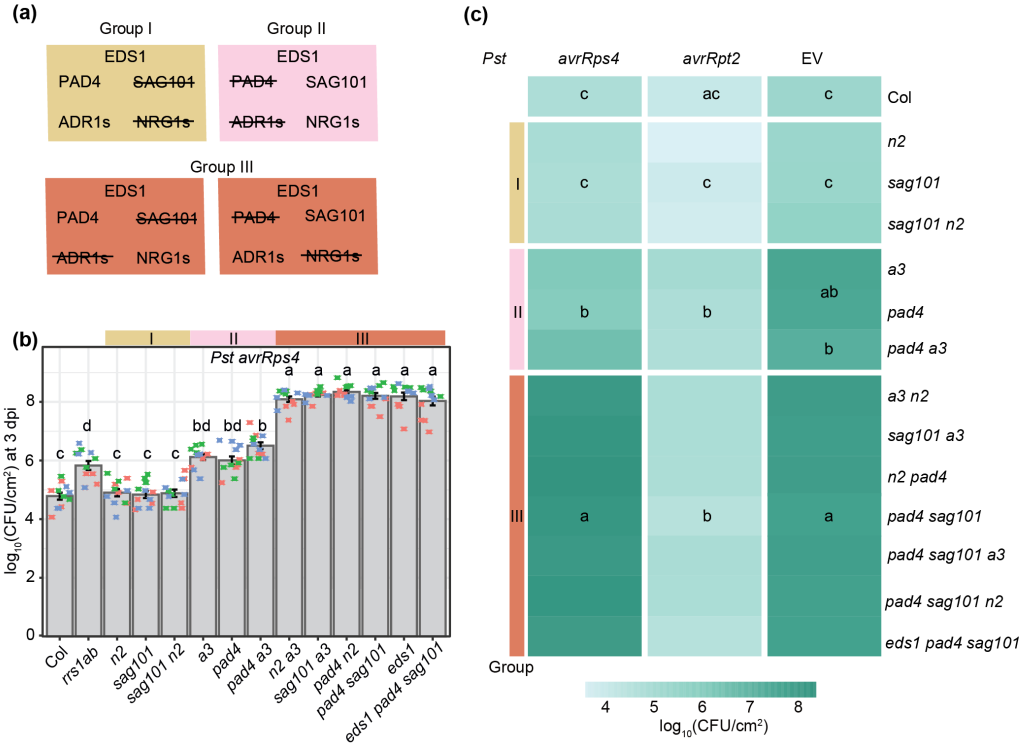

Fig. 1. Distinct *PAD4/ADR1*s and *SAG101/NRG1*s-dependent mechanisms in *Arabidopsis* TNL immunity. (a) Overview of mutants used in (b) and (c). Group I comprises mutants disabled in *SAG101* and/or *NRG1*s: *sag101*, *nrg1.1 nrg1.2* (*n2*) and *sag101 n2*. Group II has mutants in *PAD4* and/or *ADR1*s: *pad4*, *adr1 adr1-L1 adr1-L2* (*a3*) and *pad4 a3*. Group III is composed of cross-branch combinatorial mutants *a3 n2*, *sag101 a3*, *pad4 n2*, *pad4 sag101*, *sag101 pad4 a3*, *sag101 pad4 n2*, *eds1 pad4 sag101*. **(b)** Growth of *Pseudomonas syringae* pv. *tomato* DC3000 (*Pst*) *avrRps4* in leaves of *Arabidopsis* Col-0 (Col) and indicated mutants at 3 days post inoculation (dpi) via syringe infiltration (OD_{600}=0.0005). Bacterial loads are shown as $\log_{10}$ colony-forming units (CFU) per cm^2. Experiments were performed three times independently with four replicates each (Tukey's HSD, α=0.001, n=12). **(c)** Growth of *Pst avrRps4*, *Pst avrRpt2* or *Pst* (empty vector, EV) in indicated *Arabidopsis* lines at 3 dpi via syringe infiltration (OD_{600}=0.0005). Heatmap represents mean $\log_{10}$-transformed CFU values from three independent experiments, each with four replicates (n=12). Statistical significance codes are assigned based on Tukey's HSD (α =0.001, n=12). The jitter plot in (b) shows individual data points used to calculate means on the heatmap for *Pst avrRps4* infection. *sag101 a3* and *pad4 n2* phenocopy *pad4 sag101* and *a3 n2*, indicating that *SAG101* does not form functional signalling modules with *ADR1*s, and *NRG1*s with *PAD4*.

The *Arabidopsis EDS1-SAG101-NRG1*s node is dispensable for CNL^{RPS2} effector-triggered immunity

RPS2-mediated resistance to *Pst avrRpt2* was compromised only when *PAD4* or *ADR1* RNLs were mutated in group I, II and III mutants, and there was no measurable contribution of *SAG101* or *NRG1* RNLs to RPS2 immunity, even in a *pad4 a3* background (Fig. 1c). In quantitative electrolyte leakage assays we detected equivalent contributions of *PAD4* and *ADR1* RNLs to host cell death at 6 and 8 hpi, but not later at 24 hpi (Supplementary Fig. 1c), as seen previously for *pad4* and *eds1* mutants [33] and *a3* [12]. Importantly, *PAD4* and *ADR1*s early promotion of RPS2 cell death could not be substituted by *SAG101* or *NRG1*s in any of the mutant lines (Supplementary Fig. 1c). We concluded that EDS1-PAD4 also work together with ADR1s in a single pathway to promote CNL^{RPS2} -triggered early host cell death and that *SAG101* and *NRG1*s are not recruited for CNL^{RPS2} ETI, even when *PAD4* and *ADR1s* are disabled.

Next we investigated whether recruitment of *PAD4* and *ADR1*s and apparent non-utililization of *SAG101* and *NRG1*s in RPS2-triggered immunity is masked by the genetically parallel *ICS1*-dependent SA pathway [22, 32, 33, 37]. For this, we introduced an *ics1* (*sid2*) mutation into the single-module (*pad4 a3*, *sag101 n2*) and cross-module (*pad4 n2* and *sag101 a3*) mutant backgrounds (Fig. 2a). Loss of *ICS1* did not alter the different dependencies of TNL$^{RRS1-RPS4}$ or CNL^{RPS2} on *PAD4-ADR1*s and *SAG101-NRG1*s in bacterial resistance (Fig. 2a; Supplementary Fig. 2a-d). We concluded that *PAD4-ADR1*s and *SAG101-NRG1*s distinctive contributions to resistance mediated by these TNL and CNL receptors are independent of *ICS1*-generated SA.

We further tested whether a possible *SAG101* and *NRG1*s role in basal resistance against *Pst* (Fig. 1c, [12, 25]) is redundant with and therefore masked by the SA and *PAD4-ADR1*s sectors [13, 22, 38]. We found that *sag101* and *n2* mutations did not increase *sid2*, *sid2 pad4* and *sid2 a3* susceptibility to *Pst* (Fig. 2a, Supplementary Fig. 2e, f). Therefore, *SAG101* and *NRG1*s do not contribute to *Arabidopsis* resistance to *Pst* bacteria in a susceptible interaction.

Removal of the *SAG101-NRG1* and *ICS1* sectors reveals *PAD4-ADR1*s promoted TNL cell death

SAG101 and *NRG1*s are dispensible for TNL$^{RRS1-RPS4}$ resistance unless *PAD4* and/or *ADR1*s are disabled (Fig. 1b, 2a; Supplementary Fig. 2a, b), consistent with unequal contributions of these two branches in TNL immunity [12, 19, 25, 26]. We used the *Arabidopsis* combinatorial mutants with *sid2* (Fig. 2a) to explore whether *ICS1*-synthesized SA affects *PAD4-ADR1*s or *SAG101-NRG1*s involvement in TNL$^{RRS1-RPS4}$ triggered host cell death. In quantitative electrolyte leakage assays over 6 - 24 hpi and macroscopically at 24 hpi, *pad4*, *a3*, *sid2*, *pad4*

sid2 and *a3 sid2* mutants displayed similar leaf cell death responses as wild-type Col (Fig. 2 b, c). Therefore, *PAD4* and *ADR1*s are dispensable for TNL$^{RRS1\text{-}RPS4}$ cell death, regardless of *ICS1*-dependent SA status. While *n2* and *sag101* mutants had strongly reduced host cell death, as expected [12, 19, 26], we observed a cell death response similar to that of wild-type Col in *sag101 sid2* and *n2 sid2* backgrounds (Fig. 2b, c). This restored cell death was abolished in *pad4 sag101 sid2* and *a3 n2 sid2* mutants (Fig. 2b, c). We concluded that an *EDS1-PAD4-ADR1*s controlled mechanism can lead to host cell death in TNL$^{RRS1\text{-}RPS4}$ immunity that is likely antagonised or restricted by combined *EDS1-SAG101-NRG1*s and SA functions.

SA was found to conditionally suppress leaf cell death promoted by metacaspase 1 (MC1) in CNL RPM1 ETI [39], and *MC1*, *PAD4* or *ADR1*s promoted runaway cell death caused by the loss of *Lesion Simulating Disease1* (*LSD1*) [22, 40, 41, 42]. Therefore, we tested whether MC1 is required for PAD4-*ADR1*s dependent TNL$^{RRS1\text{-}RPS4}$ cell death restored in *sag101 sid2* (Fig. 2b, c). For this, we generated a *sag101 sid2 mc1* triple mutant and measured its cell death phenotype alongside *mc1* and *pad4 sid2 mc1* lines. The *mc1* mutation did not compromise *SAG101* or *PAD4* promoted TNL cell death (Supplementary Fig. 3), suggesting that *MC1* is dispensible for both *SAG101-NRG1*s- and *PAD4-ADR1*s-driven cell death outputs in TNL triggered bacterial immunity. Collectively, these data suggest that *EDS1-SAG101-NRG1*s and *EDS1-PAD4-ADR1*s are genetically hard-wired signalling modules in NLR immunity that react differently to *ICS1*-generated SA.

Figure 2

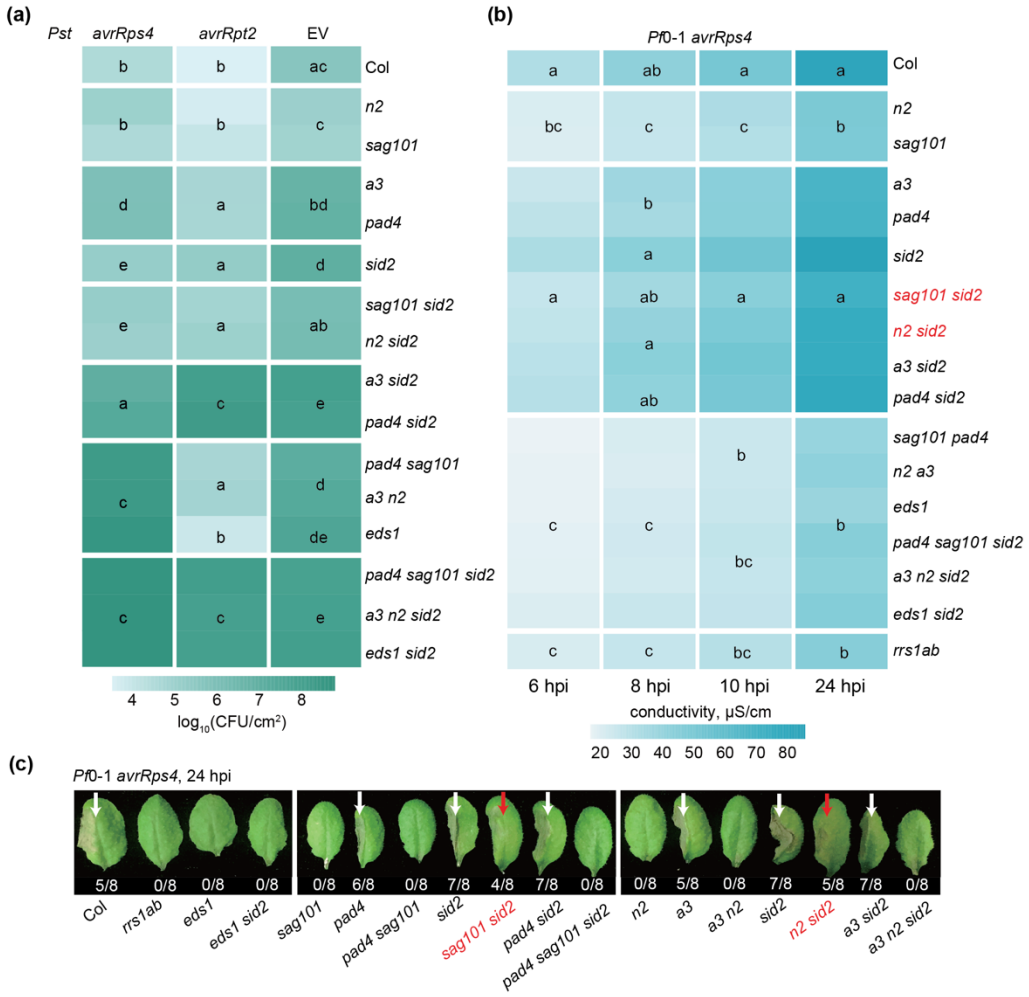

Fig. 2. *PAD4* with *ADR1*s promotion of TNL$^{RRS1\text{-}RPS4}$ cell death is exposed in lines with non-functional *ICS1* and *SAG101-NRG1*s. (a) A heatmap representation of *Pst avrRps4*, *Pst avrRpt2* or *Pst* (empty vector, EV) growth at 3 dpi in leaves of indicated genotypes (syringe infiltration OD_{600}=0.0005). The significance codes are based on the Tukey's HSD test (α=0.001, n=12-16). Data points were combined from three (*Pst avrRps4*, *Pst avrRpt2*) or four (*Pst*) independent experiments, each with four replicates. **(b)** A heatmap of quantitative cell death assays conducted on leaves of indicated genotypes after infiltration utilizing the *Pseudomonas fluorescens* 0-1 effector tester strain (hereafter *Pf*0-1) delivering *avrRps4* (OD_{600}=0.2). Cell death was measured by electrolyte leakage from bacteria-infiltrated leaf discs at 6, 8, 10 and 24 hpi. Data are displayed as means from four experiments, each with four replicates (n=16). Statistical significance codes for the difference in means are based on Tukey's HSD test (α =0.001). In mutants marked in red, the *PAD4-ADR1*s cell death branch operates in TNL$^{RRS1\text{-}RPS4}$ immunity when *SAG101-NRG1*s and *ICS1* pathways are not functional. **(c)** Visual cell death symptoms at 24 hpi *Pf*0-1 *avrRps4* infiltrating into leaf halves of indicated genotypes as in (b). The ratio beneath each leaf indicates number of leaves with visible tissue collapse from all infiltrated leaves in two independent experiments. White arrows mark cell death visible as tissue collapse in a manner dependent on *SAG101-NRG1*s. Red arrows mark cell death in lines without functional *SAG101-NRG1*s and *ICS1*.

201

202

PAD4 and SAG101 interact respectively with ADR1s and NRG1s after TNL activation in *Arabidopsis*

We tested whether the genetic co-requirement of *EDS1-PAD4-ADR1*s and *EDS1-SAG101-NRG1*s results from specific molecular associations. We generated complementing *pPAD4:YFP-PAD4* and *pSAG101:SAG101-YFP* stable transgenic lines in a Col *pad4 sag101* double mutant background (Supplementary Fig. 4) to test whether each EDS1 partner associates with similar or different RNL proteins in the TNL ETI response. These two lines and a Col *p35S:YFP-StrepII-3xHA* (YFP-SH) control were infiltrated with *Pf*0-1 *avrRps4*. *Pf*0-1 *avrRps4*-elicited leaf total soluble extracts were processed at 6 hpi because *EDS1*-dependent transcriptional reprogramming starting at ~ 4 hpi is critical for RRS1-RPS4 resistance [12, 13, 32, 43]. SAG101-YFP, YFP-PAD4 and YFP-SH proteins were purified via immunoprecipitation (IP) with GFP-trap agarose beads. Liquid chromatography and mass-spectrometry (MS) (LC-MS) analyses showed strong enrichment of the two Col-0 native EDS1A and EDS1B isoforms in both SAG101-YFP or YFP-PAD4 samples (Fig. 3a), as expected from earlier studies [30, 31, 44, 45]. EDS1A and EDS1B were also detected at a low level in YFP-SH control IPs (Fig. 3a), consistent with EDS1 weak non-specific association when its direct partners (PAD4 and SAG101) are missing [45, 46]. NRG1.1 and NRG1.2 peptides were highly enriched in SAG101-YFP but not YFP-PAD4 or YFP-SH samples. Notably, peptides derived from NRG1.3, a truncated NRG1 isoform that does not contribute genetically to TNL ETI responses [25], were enriched in SAG101-YFP IPs, and less strongly with YFP-PAD4 (Fig. 3a, Supplementary Fig. 5). By contrast, ADR1-L1 and ADR1-L2 co-purified with YFP-PAD4 but were not detected in SAG101-YFP or YFP-SH IP samples (Fig. 3a, Supplementary Fig. 5), suggesting that ADR1 group RNLs interact preferentially with PAD4 over SAG101 at 6 hpi. Put together, the *Arabidopsis* IP-MS analyses show that EDS1-PAD4 and EDS1-SAG101 dimers interact specifically with RNLs in TNL-induced tissues at 6 hpi. The observed preferential association of PAD4 with ADR1-L1 and ADR1-L2, and SAG101 with NRG1.1 and NRG1.2, further suggests that EDS1-PAD4 and EDS1-SAG101 associations with specific helper RNL types underpin these genetically distinct *Arabidopsis* immunity modules.

Figure 3

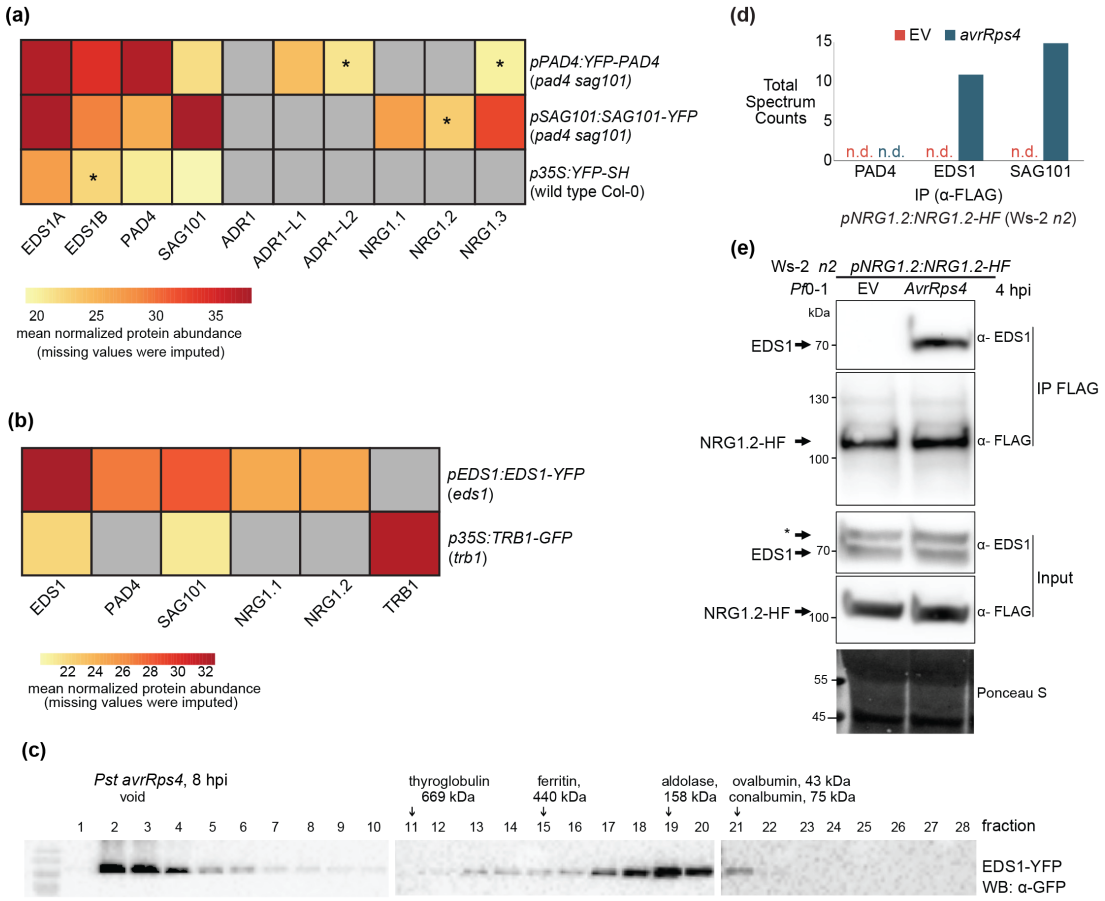

Fig. 3. Early effector-dependent NRG1 association with EDS1 and SAG101 in Arabidopsis TNL$^{RRS1\text{-}RPS4}$ triggered ETI. **(a)** Heat map of normalized abundance values (LFQ, log_2-scaled) for proteins detected in liquid chromatography mass-spectrometry (LC-MS) analyses after α-GFP immunoprecipitation (IP) of PAD4-YFP or SAG101-YFP from total leaf extracts of respective complementation lines *pPAD4:YFP-PAD4* and *pSAG101:SAG101-YFP* (both Col *pad4 sag101* background) after infiltration with *Pf*0-1 *avrRps4* (6 hpi, OD_{600}=0.2). ADR1s are specifically enriched in YFP-PAD4 IP samples, whereas NRG1s are more abundant in the SAG101-YFP IP samples. Samples were collected from four independent experiments. All protein values shown $|\Delta log_2 LFQ| \geq 1$, $p \leq 0.05$ (relative to YFP-SH IP). Asterisks indicate detection in three of four replicates. Grey indicates not detected or detected in < 3 of 4 replicates. **(b)** Heat map of LFQ values for proteins detected in LC-MS analyses after IP of EDS1-YFP and TRB1-GFP from nuclei-enriched extracts of corresponding *Arabidopsis* complementation lines (García et al., 2010; Zhou et al., 2016) infiltrated with *Pst avrRps4* (8 hpi, OD_{600}=0.1). NRG1.1 and NRG1.2 are specifically enriched in EDS1-YFP samples. Samples were collected from four independent experiments. All shown protein $|\Delta log_2 LFQ| \geq 1$, $p \leq 0.05$ (relative to TRB1-GFP IP). Grey means the protein is not detected or detected in <3 of 4 replicates.(c) α-GFP probed immunoblots of nuclei-enriched extracts from leaves of the *Arabidopsis pEDS1:EDS1-YFP* complementation line (Col *eds1* background) infiltrated with *Pst avrRps4* (OD_{600}=0.1, 8 hpi). Extracts were resolved using native gel filtration. Arrows below protein markers indicate position of the corresponding peak. Numbers refer to column fractions. EDS1 forms stable ~100-600 kDa complexes. The experiment was repeated three times with similar results. (d) LC-MS analysis of eluates after α-FLAG IP of total leaf extracts from Arabidopsis Ws-2 *n2 pNRG1.2:NRG1.2-HF* complementation line (Castel et al., 2019) infiltrated with *Pf*0-1 *EV* or *Pf*0-1 *avrRps4* (4 hpi, OD_{600}=0.3). Peptides corresponding to EDS1 and SAG101 were observed in eluates only after *Pf*0-1 mediated delivery of avrRps4. This result was observed in two independent experiments. (e) Immunoblot analysis of eluates from (d). Asterisk indicates a nonspecific band on the α-EDS1 blot for input samples. The analysis was performed on total leaf extracts and was repeated four times with similar results. Association of EDS1 with NRG1.2-HF was observed only after *Pf*0-1-mediated delivery of avrRps4. Ponceau S staining shows equal protein loading in input samples on the blot.

232

233

Early effector dependent NRG1 association with EDS1 and SAG101 in *Arabidopsis*

To investigate whether the RNLs associate with EDS1, we enriched for EDS1 protein from a transgenic Col *eds1* line expressing *pEDS1:EDS1-YFP* [43] at 8 h after infiltrating leaves with *Pst avrRps4* bacteria and preparing nuclear-enriched extracts. Garcia et al (2010) demonstrated the importance of an EDS1 nuclear pool for gene expression reprogramming in TNL$^{RRS1\text{-}RPS4}$ triggered ETI [43]. To interrogate protein associations with EDS1, we immunoprecipitated EDS1-YFP using GFP-trap agarose beads and analyzed co-purifed proteins via LC-MS. GFP-trap purification and LC-MS processing of eluates from a Col mutant in *Telomere Repeat Binding 1* (*TRB1*) expressing nuclear localized TRB1-GFP [47] was used as a control for non-specific associations (Fig. 3b, Supplementary Fig. 6). PAD4 and SAG101 were highly enriched in EDS1-YFP relative to TRB1-GFP pulldowns, as represented in a volcano plot (Supplementary Fig. 6), and consistent with EDS1 stable PAD4 or SAG101 dimers persisting in a TNL$^{RRS1\text{-}RPS4}$ ETI response [44, 45]. NRG1.1 and NRG1.2 proteins were also specifically enriched in EDS1-YFP compared to TRB1-GFP samples (Fig. 3b). We did not detect any of the three functional *Arabidopsis* ADR1 isoforms, ADR1, ADR1-L1 and ADR1-L2 [22] (Fig. 3b). In the nuclei-enriched protein extracts separated by native size exclusion chromatography, EDS1-YFP eluted between ~50 and ~600 kDa (Fig. 3c). An EDS1-YFP peak at ~160 kDa with a higher molecular weight tail is consistent with EDS1 forming stable exclusive heterodimers with PAD4 or SAG101 [30, 31, 45] and sub-stoichiometric higher order complexes (Fig. 3c). Together, these data suggest that NRG1.1 and NRG1.2 also interact with EDS1 in TNL$^{RRS1\text{-}RPS4}$ activated cells.

We also tested whether the association of NRG1 group RNLs with EDS1 and SAG101 is dependent on TNL$^{RRS1\text{-}RPS4}$ activation using an *Arabidopsis* Ws-2 *n2* complementation line expressing *pNRG1.2:NRG1.2-6xHis-3xFLAG* (*NRG1.2-HF*) [19]. Leaves were infiltrated with *Pf*0-1 bacteria delivering avrRps4 (*Pf*0-1 *avrRps4*) to activate RRS1-RPS4 ETI or *Pf*0-1 with an empty vector (EV) as a negative control eliciting PTI [48, 49]. Soluble extracts from *Pf*0-1 EV and *Pf*0-1 *avrRps4*-infiltrated leaves at 4 hpi were processed to monitor early changes during the *EDS1*-dependent transcriptional reprogramming in TNL$^{RRS1\text{-}RPS4}$ resistance [12, 13, 32, 43, 49]. After NRG1.2-HF immunopurification on α-FLAG agarose beads, LC-MS analysis revealed spectra for peptides derived from EDS1 and SAG101 in elution products isolated from *Pf*0-1 *avrRps4* but not *Pf*0-1 (EV) treated tissues (Fig. 3d). Notably, no PAD4 peptides were identified in the analysis. Elution products resolved by SDS-PAGE and probed with α-FLAG and α-EDS1 antibodies also revealed an association of EDS1 with NRG1.2, dependent upon *Pf*0-1 delivery of avrRps4 (Fig. 3e). Importantly, no association between NRG1.2 and EDS1 or SAG101 was detected at 4 hpi with *Pf*0-1 alone, indicating that a PTI response [15, 16, 50] is insufficient to induce NRG1 association with EDS1 and SAG101 (Fig 3d, e). These data show

that $TNL^{RRS1\text{-}RPS4}$ activation induces NRG1.2 associations with EDS1 and SAG101, but not PAD4, in *Arabidopsis*.

XopQ/Roq1-dependent *Arabidopsis* NRG1.1 association with EDS1 and SAG101 in *N. benthamiana*

Previously, transient co-expression of *Arabidopsis* EDS1, SAG101 and NRG1.1 or NRG1.2 proteins in an *N. benthamiana* CRISPR *eds1a pad4 sag101a sag101b* (*Nb-epss*) mutant reconstituted host cell death and bacterial resistance after TNL^{Roq1} recognition of the bacterial effector XopQ [26, 51]. We exploited the *Nb-epss* transient assay system to investigate molecular requirements for *Arabidopsis* EDS1, SAG101, NRG1s associations and functions in ETI. For this, we developed an ETI assay in *Nb-epss* leaves with more precise timing of the TNL^{Roq1} dependent response than previously achieved using only *Agrobacteria*-mediated expression of various components [26]. In the modified assay, we transiently expressed combinations of epitope tagged proteins into *Nb-epss* leaf zones using *Agrobacteria* and, after 48 h, infiltrated *Pf*0-1 *XopQ* bacteria to activate TNL^{Roq1} immunity (Fig. 4a). Co-expression of *Arabidopsis* EDS1-FLAG, SAG101-FLAG and NRG1.1-SH led to XopQ-dependent host cell death quantified in electrolyte leakage assays at 24 hpi (Fig. 4b). In this ETI assay, replacement of *Arabidopsis* NRG1.1-SH by ADR1-L2-SH or co-expression of GUS-FLAG with NRG1.1-SH did not lead to XopQ triggered host cell death (Fig. 4b), consistent with PAD4 being dispensable for TNL immune responses in *N. benthamiana* [26, 29], even with a *Pf*0-1 stimulus.

Figure 4

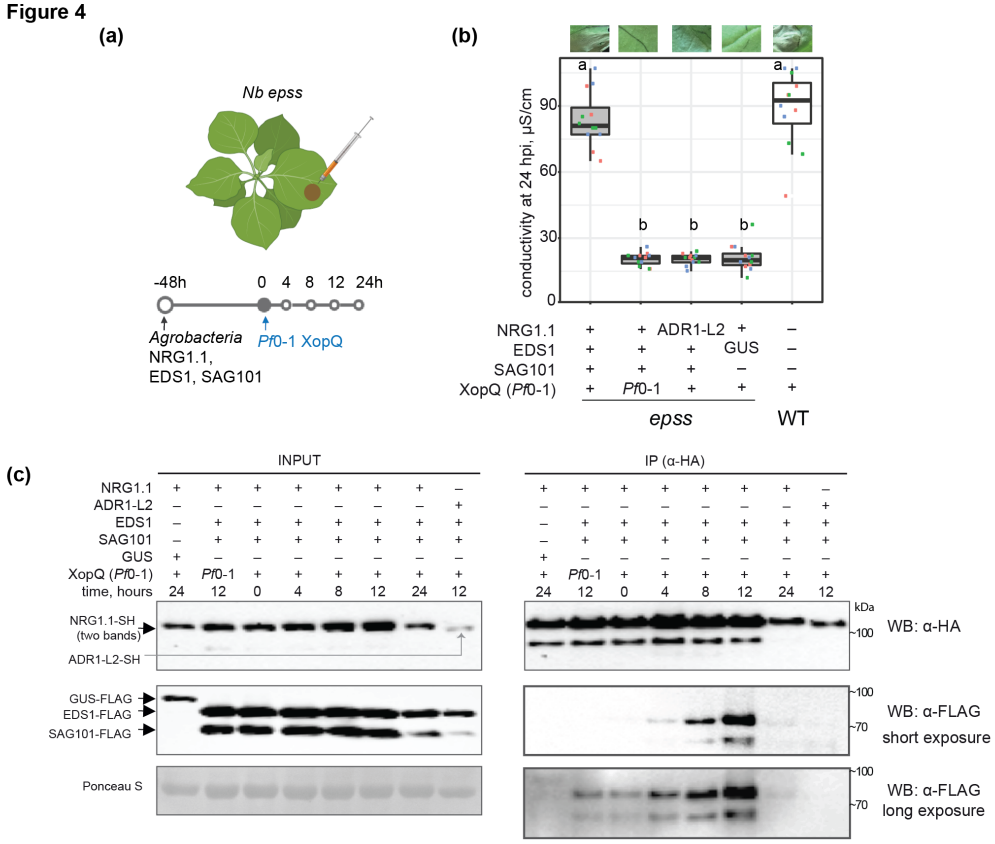

Fig. 4. TNL^{Roq1} effector recognition-dependent *Arabidopsis* NRG1 association with EDS1 and SAG101 in *N. benthamiana*. (a) Sample collection scheme for experiments in (b) and (c). Roq1-dependent cell death is restored in the *Nb eds1 pad4 sag101a sag101b* (*Nb-epss*) signalling deficient mutant by expressing *Arabidopsis* EDS1, SAG101 and NRG1.1 via *Agrobacteria* infiltration 48 h before XopQ effector delivery. *Pf*0-1 *XopQ* is syringe-infiltrated (OD_{600}=0.3) to deliver the effector in a time-resolved manner and study TNL signalling events up to 24 hpi. (b) Macroscopic symptoms and quantification of XopQ-triggered cell death at 24 hpi after infiltrating *Pf*0-1 *XopQ* in leaves of *Nb-epss* expressing *Arabidopsis* EDS1-FLAG, SAG101-FLAG, NRG1.1-3xHA-StrepII (NRG1.1-SH) or ADR1-L2-3xHA-StrepII (ADR1-L2-SH). *Pf*0-1 served as a "no-ETI" control. Cell death was quantified in electrolyte leakage assays 6 h after harvesting leaf discs (24 hpi with *Pf*0-1 *XopQ*). The experiment was performed three times independently, each with four technical replicates (leaf discs) (Tukey's HSD, α=0.001, n=12). Transiently expressed Arabidopsis EDS1, SAG101 and NRG1.1 proteins are functional in *Pf*0-1 *XopQ* triggered (Roq1) cell death. (c) Coimmunoprecipitation assay followed by Western blotting to test for XopQ-triggered associations between Arabidopsis NRG1.1-SH and FLAG-tagged EDS1 or SAG101 in *Nb-epss* according to the infiltration scheme in (a). NRG1.1-SH or ADR1-SH were enriched using α-HA agarose beads, and presence of FLAG-tagged EDS1, SAG101 or GUS was tested by probing blots with α-FLAG antibodies. IP assays were repeated three times independently with similar results. NRG1.1 association with EDS1 and SAG101 requires Roq1/XopQ ETI activation.

290

291

We performed a time course to monitor the accumulation and associations of NRG1.1-SH with EDS1-FLAG and SAG101-FLAG in *Nb-epss* leaf samples harvested at 4, 8, 12 and 24 h after *Pf*0-1 *XopQ* inoculation. Although protein inputs were similar in all samples, NRG1.1-SAG101 and NRG1.1-EDS1 association was detected in α-HA immunopurified samples only at 8 and 12 hpi with *Pf*0-1 *XopQ* (Fig. 4c). The immunoprecipitation (IP) signals were no longer detectable at 24 hpi, suggesting that *Pf*0-1 *XopQ* induced NRG1 association with EDS1 and SAG101 is transient and/or disrupted by host cell death at 24 hpi (Fig. 4b, c). As in *Arabidopsis*, no association between NRG1.1 and EDS1 or SAG101 was detected at 12 hpi with *Pf*0-1 alone (Fig. 4c), further indicating that a PTI response in *N.benthamiana* is insufficient to induce NRG1 association with EDS1 and SAG101. Similarly, when *Arabidopsis* ADR1-L2-SH was expressed instead of NRG1.1-SH in the *Nb-epss* TNL^{Roq1} ETI assay, it did not interact with SAG101-FLAG or EDS1-FLAG at 12 hpi (Fig. 4c), mirroring the failure of ADR1-L2 to signal Roq1-triggered host cell death or bacterial resistance in *N. benthamiana* (Fig. 4b; [26]). These data show that XopQ activation of TNL^{Roq1} in *Nb-epss* leaves is necessary to induce NRG1.1 association with SAG101 and EDS1 proteins from *Arabidopsis*. The similarity between *Arabidopsis* EDS1 family protein associations with RNLs observed in native *Arabidopsis* (Fig. 3) and non-native *N. benthamiana* (Fig. 4) suggests that interaction specificity determines function of *Arabidopsis EDS1-SAG101-NRG1*s module in TNL immunity. Analyses in both systems also show that a PTI stimulus alone is insufficient for NRG1 association with EDS1 and SAG101.

Effector-dependent *Arabidopsis* NRG1 association with EDS1 and SAG101 requires a functional EDS1 EP domain

Assembly of *Arabidopsis* EDS1 heterodimers with PAD4 or SAG101 is mediated by a short N-terminal EDS1 α-helix (αH) fitting into an N-terminal hydrophobic groove of either partner [30, 32, 46]. Protein structure-function studies of *Arabidopsis* and tomato EDS1-SAG101 complexes showed that the heterodimer brings into close proximity two α-helical coils (EDS1 αP and SAG101 αN) on the partner C-terminal 'EP' domains, which are essential for TNL ETI signalling [26, 29, 30, 32]. *Arabidopsis* EDS1 residues F419 and H476 are positioned close to SAG101 αN in the dimer cavity (Fig. 5a) [26]. In earlier *Agrobacteria*-only based *Nb-epss* reconstitution assays, an *Arabidopsis* EDS1^{F419E} mutation disabled TNL^{Roq1} signalling without disrupting the EDS1-SAG101 heterodimer [26]. In the *Agrobacteria* plus *Pf*0-1 *XopQ* TNL^{Roq1} assay (Fig. 4a), *Arabidopsis* EDS1^{F419E}-FLAG and EDS1^{H476Y}-FLAG single amino acid exchange variants failed to mediate XopQ/Roq1-dependent host leaf cell death at 24 hpi or *Xanthomonas euvesicatoria* (formerly, *Xanthomonas campestris* pv. *vesicatoria*, *Xcv*) growth at 6 dpi (Fig. 5b, c). Also, substituting NRG1.1-SH with ADR1-L2-SH did not confer TNL^{Roq1}-triggered host cell death and *Xcv* resistance (Fig. 5b, c). We monitored the expression of

328 FLAG-tagged EDS1 family proteins by immunoblotting and performed NRG1.1-SH α-HA IP
329 assays on *Pf*0-1 *XopQ* triggered leaf protein extracts at 10 - 12 hpi when TNL-induced
330 NRG1.1-EDS1 and NRG1.1-SAG101 associations were strongest (Fig. 4c). As negative
331 controls, PAD4-FLAG was substituted for SAG101-FLAG, GUS-FLAG for EDS1-FLAG, and
332 ADR-L2-SH for NRG1.1-SH (Fig. 5d). While all proteins were detected in input samples,
333 NRG1.1 was detected only when NRG1.1-SH was co-expressed together with functional wild-
334 type EDS1-FLAG and SAG101-FLAG (Fig. 5d). The failure of NRG1.1 to IP SAG101 with GUS
335 replacing EDS1 (Fig. 5d), indicates that NRG1.1 associates specifically with the EDS1-
336 SAG101 heterodimer and not individual EDS1 or SAG101 monomers, upon triggering of
337 TNL^{Roq1} ETI. The strong reduction in NRG1.1 association with EDS1 EP domain inactive
338 variants $EDS1^{F419E}$ or $EDS1^{H476Y}$ shows that NRG1 fails to associate with a signalling-inactive
339 EDS1-SAG101 heterodimer after Roq1 activation.

340

Figure 5

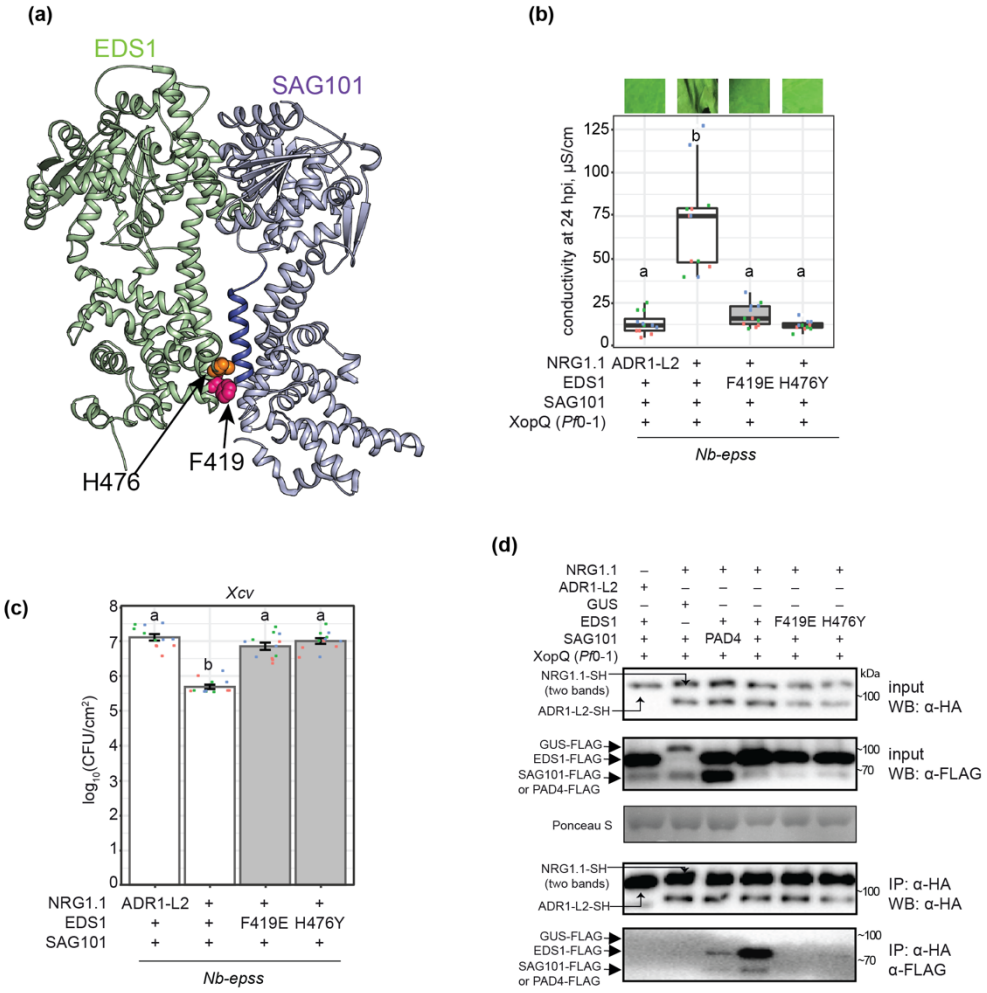

Fig. 5. Effector-dependent NRG1-EDS1-SAG101 association requires a functional EDS1 EP domain. (a) Representation of the *Arabidopsis* EDS1 (green) - SAG101 (purple) heterodimer crystal structure (PDB: 4NFU) with highlighted EP-domain cavity surfaces that are essential for TNL triggered cell death (Lapin et al., 2019). An α-helix of the SAG101 EP domain (blue) and residues F419 (magenta) and H476 (orange) in the EDS1 EP domain are shown as ribbon and spheres, respectively. **(b,c)** Roq1/XopQ-dependent cell death (b) and bacterial resistance (c) in leaves of *Nb-epss* transiently expressing of C-terminally FLAG-tagged EDS1 wildtype and mutant variants with SAG101-FLAG and NRG1.1-SH or ADR1-L2-SH. Cell death was triggered by infiltrating *Pf*0-1 *XopQ* at 48 h after *Agrobacteria* infiltration to express the *Arabidopsis* proteins; photos of leaf discs for the electrolyte leakage assays were taken at 24 h. Roq1 resistance to *Xanthomonas campestris* pv. *vesicatoria* (*Xcv*) strain 85-10 expressing XopQ. F419E and H476Y mutations in the Arabidopsis EDS1 EP domain abrogated cell death and resistance, as shown in (Lapin et al., 2019) using different plasmid backbones and tags. Experiments were performed three times independently, each with four replicates (leaf discs) (Tukey's HSD, α=0.001, n=12). **(d)** IP followed by Western blot analysis to test dependency of associations between *Arabidopsis* EDS1-SAG101 and NRG1.1 in *Nb-epss* on a functional EDS1 EP domain cavity. Leaves of Nb-epss were infiltrated with *Agrobacteria* to express FLAG-tagged EDS1 or its variants EDS1F419E and EDS1H476Y, SAG101-FLAG and NRG1.1-SH or PAD4-FLAG, with ADR1-L2-SH and GUS-FLAG as negative controls. At 2 dpi, *Pf*0-1 *XopQ* (OD_{600}=0.3) was infiltrated, and the triggered samples were collected at 10 hpi. Following IP with α-HA agarose beads, input and and IP fractions were probed with α-HA and α-FLAG antibodies. Roq1/XopQ-dependent association of NRG1.1-SH with EDS1-FLAG and SAG101-FLAG was abolished in samples with mutated EDS1 EP domain variants. Similar results were obtained in three independent experiments.

N-terminal residues of *Arabidopsis* NRG1 associating with EDS1 and SAG101 are essential for signalling

We next examined NRG1 molecular features that might influence its TNL signalling function and association with EDS1-SAG101. Because RNLs have domain architectures similar to sensor CNL proteins [17], we modeled NRG1.1 onto the cryo-EM structure of the activated *Arabidopsis* CNL receptor ZAR1 which forms a pentameric resistosome [7]. The ZAR1 signalling active pentamer has five exposed N-terminal α-helices (α1) preceding the CC domains of the NLR protomers, which assemble into a potential membrane associated pore or channel [7]. Structural modelling of *Arabidopsis* NRG1.1 identified two negatively charged N-terminal glutamic acid (E) residues (E14 and E27) (Fig. 6a) positioned similarly to ZAR1 α1-helix residues E11 and E18 that are part of the ZAR1 inner funnel and are necessary for ZAR1 resistosome activity [7]. Two other NRG1.1 N-terminal residues, leucine 21 (L21) and lysine 22 (K22) (Fig. 6a), aligned with L10 and L14 in the ZAR1 α1-helix which promoted ZAR1 membrane association and resistosome signalling [7]. Neither set of ZAR1 α1-helix amino acids was required for effector induced pentamer assembly [7]. We further identified in *Arabidopsis* NRG1 RNLs the conserved NLR nucleotide-binding domain (NBD) P-loop (GxxxxGK(T/S)) motif ($G^{199}K^{200}T^{201}$ in *Arabidopsis At*NRG1.1; Fig. 6a; Supplementary Fig. 7), which mediates nucleotide binding [52, 53], and induced self-association and/or signalling functions of several sensor NLRs [54, 55]. The P-loop was dispensable for ADR1-L2 conferred resistance during ETI and basal immunity and NRG1.1 conditioned TNL *chs3-2D* auto-immunity [22, 25], but was required for ADR1-L2 conditioned *lsd1* mediated cell death and *NRG1* dependent TNL^{Roq1} immunity [35, 41].

Figure 6

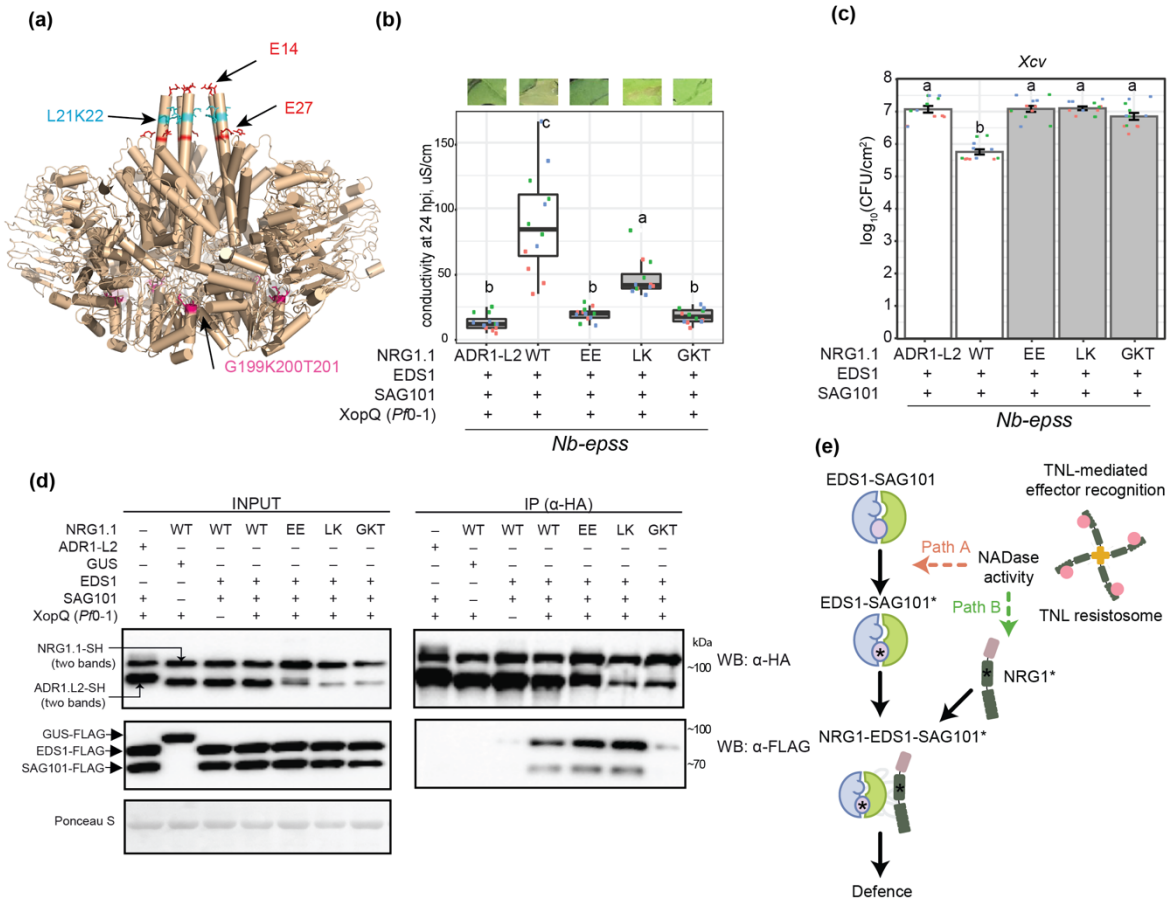

Fig. 6. Association between *Arabidopsis* NRG1.1, EDS1 and SAG101 requires an intact NRG1.1 P-loop. (a) A structure homology model of *Arabidopsis* NRG1.1 based on the ZAR1 resistosome (PDB: 6J5T, chains G-O). NRG1.1 amino acids E14 and E27 (red sticks) and L21 and K22 (blue sticks) are predicted to align with functionally defined residues E11, E18, F9, L10 and L14 in the N-terminal ZAR1 α1-helix. The modelled NRG1.1 P-loop motif (G199 K200 T201) is shown as cyan sticks. *Pf*0-1 *XopQ*-triggered cell death **(b)** and bacterial (*Xcv*) growth restriction **(c)** in *Nb-epss* expressing *Arabidopsis* NRG1.1-SH wildtype, NRG1.1$^{E14A/E27A}$, NRG1.1$^{L21A/K22A}$ and NRG1.1$^{G199A/K200A/T201A}$ variants together with EDS1-FLAG and SAG101-FLAG. *Arabidopsis* proteins were expressed via *Agrobacteria*-mediated transient expression assays 2 d before *Pf*0-1 *XopQ* (OD_{600}=0.3) or simultaneously with *Xcv* (OD_{600}=0.0005) infiltration. An intact NRG1.1 predicted N-terminal α-helix and P-loop are required for NRG1.1 function in reconstituted ETI^{Roq1} cell death and pathogen resistance. Experiments were performed three times independently, each with four technical replicates (leaf discs) (Tukey's HSD, α=0.001, n=12). **(d)** IP and Western blot analyses testing associations of *Arabidopsis* NRG1.1 mutant variants with EDS1 and SAG101 in *Nb-epss* after triggering Roq1 signalling by *Pf*0-1 *XopQ* infiltration (OD_{600}=0.3; 10 hpi). *Arabidopsis* EDS1-FLAG, SAG101-FLAG with NRG1.1-SH, and using GUS-FLAG and *Arabidopsis* ADR1-L2-SH as negative controls, were expressed using *Agrobacteria* 2 d prior to *Pf*0-1 *XopQ* infiltration. After α-HA IP, the indicated fractions were analyzed with α-HA and α-FLAG antibodies by Western blotting. An NRG1.1 intact P-loop but not N-terminal amino acids are essential for Roq1/XopQ-dependent NRG1.1 association with the EDS1-SAG101 dimer. The experiment was repeated three times independently with similar results. **(e)** Model of molecular events leading to generation of an Arabidopsis EDS1-SAG101-NRG1 signalling complex that is essential for TNL receptor activated defence. NRG1-EDS1-SAG101 association is dependent on TNL-effector activation and requires an intact EDS1-SAG101 heterodimer EP domain cavity (purple circle) and NRG1 nucleotide binding domain P-loop motif. In two depicted scenarios, an effector-induced TNL oligomer with NADase activity leads to activation (asterisks) of EDS1-SAG101 via the EP domain cavity ('Path A', asterisk inside the purple circle) or NRG1 ('Path B'). These paths are not mutually exclusive. EDS1-SAG101-NRG1 assembly precedes and is necessary for TNL triggered cell death and resistance involving a predicted NRG1 N-terminal HeLo domain α-helix.

366

367

We made amino acid exchanges to alanines in the NRG1.1 predicted α1-helix E11/E27 (denoted EE) and L21/L22 (LK) pairs and a non-functional NRG1.1 $G^{199}K^{200}T^{201}$/AAA P-loop variant (denoted GKT). When co-expressed with *Arabidopsis* EDS1 and SAG101 in the *Nb-epss* TNL^{Roq1}assay, $NRG1.1^{EE}$ and $NRG1.1^{GKT}$ variants were non-functional and $NRG1.1^{LK}$ was partially functional in eliciting host cell death (Fig. 6b). All mutant NRG1.1-HA variants failed to confer *Xcv* resistance (Fig. 6c). The NRG1.1-HA variants were detected on immunoblots, as were co-expressed EDS1-FLAG and SAG101-FLAG proteins (Fig. 6d; left panel). In NRG1.1 α-HA IP assays, the NRG1.1-HA N-terminal EE and LK mutants immunoprecipitated EDS1-FLAG and SAG101-FLAG as efficiently as wild-type NRG1.1-SH (Fig. 6d; right panel). By contrast, the NRG1.1 P-loop GKT mutant displayed a much weaker association with EDS1 and SAG101 (Fig. 6d; right panel). Failure of $NRG1.1^{GKT}$ to interact with EDS1 and SAG101 indicates a requirement for ADP/ATP binding and/or nucleotide exchange at the NRG1.1 nucleotide binding domain for TNL induced association with EDS1-SAG101 and immunity. Retention of $NRG1.1^{EE}$ and $NRG1.1^{LK}$ TNL induced association with EDS1-SAG101, but their loss of immunity activity, suggests that an intact NRG1.1 N-terminal putative α-helix is required for NRG1 signalling in TNL ETI as part of or after TNL-induced association with EDS1-SAG101.

Discussion

Plant intracellular NLR receptors, activated directly or indirectly by pathogen effectors, provide a critical surveillance mechanism against disease. Activated forms of the two major sensor NLR classes, TNLs and CNLs, assemble into oligomers that are required for immunity signalling and broadly resemble mammalian NLR inflammasome scaffolds [7, 8, 9, 56]. Two phylogenetically related groups of HeLo domain helper NLRs (NRG1s and ADR1s) and the EDS1 family of plant-specific lipase-like proteins (EDS1, PAD4 and SAG101) mediate signalling downstream of sensor NLRs, leading to transcriptional defences and localised host cell death [19, 25, 26, 28, 35].

Here we provide genetic and molecular evidence in *Arabidopsis* that distinct RNL immunity modules (or branches) operate with specific EDS1 family heterodimers. The two modules contribute in different ways to $TNL^{RRS1\text{-}RPS4}$ and CNL^{RPS2} ETI, and to basal immunity against virulent bacteria (Fig. 1 and 2; Supplementary Fig. 1-3). We show in *Arabidopsis* and *N. benthamiana* that TNL-effector activation induces a specific association between NRG1 proteins and EDS1-SAG101 heterodimers (Fig. 3 and 4). In *N. benthamiana* TNL ETI reconstitution assays, interactions of NRG1 with EDS1 and SAG101 and effective TNL immunity signalling require a functional EDS1 EP domain within the EDS1-SAG101

heterodimer and an intact P-loop motif in NRG1 for nucleotide binding (Fig. 5 and 6). Conserved amino acids at the NRG1 N-terminus, modelled onto the structure of a CNL receptor (ZAR1) membrane pore-forming α1-helix [7], are important for TNL ETI but not for TNL-induced NRG1 association with EDS1-SAG101 (Fig. 6). Our data provide a first molecular underpinning for genetically separate RNL-EDS1 mechanisms conferring immunity and cell death downstream of NLR-mediated effector recognition (Fig. 1 and 2; [25, 26, 28]). The data further demonstrate that sensor NLR-induced assembly of helper NLRs with EDS1 family proteins is a critical step for TNL downstream signalling.

Previous studies in *Arabidopsis* revealed unequal genetic and transcriptional contributions (unequal redundancy) of *PAD4* vs. *SAG101* [19, 25, 26, 31] and *ADR1* vs. *NRG1* groups in ETI and basal immunity responses to pathogens [12, 26]. *Arabidopsis SAG101* and *NRG1*s function in ETI mediated by TNL receptors and are drivers of TNL host cell death and transcriptional reprogramming [12, 26, 27]. *PAD4* and *ADR1*s are recruited more broadly for TNL and CNL ETI immune responses, in which they control transcriptional SA-dependent and SA-independent defence pathways [22, 28, 32, 33]. Our analysis of *Arabidopsis pad4, sag101, adr1- and nrg1*-group combinatorial mutants shows that individual components of the two immunity modules are not interchangeable in TNL$^{RRS1\text{-}RPS4}$ or CNL^{RPS2} immune responses. These data reveal a specificity in module composition and function (Fig. 1, Supplementary Fig. 1).

Removal of the *ICS1*dependent SA pathway uncovered the extent to which separate *PAD4-ADR1*s and *SAG101-NRG1*s genetic mechanisms are preserved (Fig. 2 and Supplementary Fig. 2). The SA pathway is bolstered in *Arabidopsis* by *PAD4* and *ADR1*s via a mutually reinforcing feedback loop [22, 33, 41, 57]. Notably, the removal of *ICS1* and *SAG101* together, released a *PAD4-ADR1*s activity leading to host cell death in TNL$^{RRS1\text{-}RPS4}$ immunity (Fig. 2b, c). Hence, each TNL signalling branch has a transcriptional reprogramming and cell death-inducing capacity, depending on the status of other pathways in the network [5, 58, 59]. *SAG101-NRG1*s and SA antagonism of *PAD4-ADR1*s stimulated cell death suggests there is crosstalk between the different sectors, possibly to limit host tissue damage and promote systemic relay of immunity signals [28]. Although metacaspase 1 (MC1) controlled proteolysis promoting RPM1 cell death is also conditionally antagonized by SA [39], we did not detect a role for *MC1* in *SAG101-NRG1*s or *PAD4-ADR1*s stimulated TNL$^{RRS1\text{-}RPS4}$ triggered cell death (Supplementary Fig. 3).

Arabidopsis IP-LC-MS analyses using EDS1, SAG101, PAD4 and NRG1.2 individually as baits were performed in TNL$^{RRS1\text{-}RPS4}$ triggered leaf tissues between 4 and 8 h after bacterial infiltration, based on knowledge of a critical 4-8 h time window needed for EDS1-PAD4 and ADR1s mobilized gene expression to be effective in immunity [12, 13, 32, 43, 49]. Also, *Arabidopsis*

TNL$^{RRS1\text{-}RPS4}$ triggered *SAG101-NRG1*s-dependent cell death started to increase from 6-8 hpi with *Pf*0-1 *avrRps4* (Fig. 1 and 2; Supplmentary Fig. 1; [26]). The sum of IP-MS data (Fig. 3) point to molecular specificity in EDS1-SAG101 association with NRG1.1 and NRG1.2 functional isoforms, and in EDS1-PAD4 association with ADR1-L1 and ADR-L2 isoforms, in TNL receptor induced cells. The absence of a detectable association between NRG1.2 with EDS1 or SAG101 at 4 h after *Pf*0-1 EV treatment (Fig. 3d), shows that PTI alone is insufficient to induce NRG1s associations with EDS1 or SAG101. These data imply that NRG1.2 association with EDS1 and SAG101 requires an activated TNL-derived signal. We suggest it is likely that an EDS1-SAG101-NRG1 functional interaction is principally a post-transcriptional event because (i) it was detected in *Arabidopsis* at 4 hpi (Fig. 3d, e) before the main *EDS1*-dependent transcriptional elevation at 8-10 hpi [12, 32, 49] and (ii) it could be recapitulated in *N. benthamiana* with abundant transiently expressed proteins only after an effector-TNL trigger (Fig. 4c).

Interestingly, a signalling inactive truncated NRG1.3 isoform [25] was enriched with both SAG101 and to a lesser extent with PAD4 (Fig. 3a). This might reflect an NRG1.3 role in negative regulation of both modules. It is also possible that NRG1 determinants for preferential association with EDS1-SAG101 lie in the NRG1 C-terminal portion. Weak association detected between PAD4 and NRG1.1 (Fig. 5d) also deviates from otherwise clear-cut specific associations of within-module components (Fig. 3a). However, these associations are unlikely to contribute to *Arabidopsis* TNL immune signalling (Fig. 1; [26]).

We interrogated the molecular requirements for *Arabidopsis* EDS1 and SAG101 functional association with NRG1.1 in *Nb-epss* TNL^{Roq1} transient reconstitution assays. TNL ETI induced NRG1.1 association was only observed in IPs with EDS1 and SAG101 together (Fig 4c, 5d, 6d), supporting NRG1 association with a signalling competent EDS1-SAG101 heterodimer (Fig. 3) but not with EDS1 or SAG101 individually (Fig. 5d) which are inactive [30, 45, 46]. A previous study proposed that NRG1 signals downstream of EDS1 in regulating TNL^{Roq1} immunity and cell death [35]. Our protein interaction assays instead point to NRG1 working biochemically together with EDS1-SAG101 in the TNL^{Roq1} immunity signalling cascade. The discrete timing of NRG1-EDS1-SAG101 association detection between 8-12 hpi suggests it is transient in nature, although it is unclear in this system whether reduced association at later time-points is a controlled event, possibly to dampen outputs, or due to cell death.

A requirement for EDS1 EP domain essential residues within the EDS1-SAG101 heterodimer [26, 29] to interact with NRG1.1 in a TNL ETI-dependent manner (Fig. 5d), suggests that an intact EDS1-SAG101 EP-domain drives its association with NRG1 downstream of TNL receptor activation, as depicted in a model (Fig. 6e). Notably, the TNL-induced NRG1-EDS1-SAG101

association and ETI also required a nucleotide-binding form of NRG1.1, whereas N-terminal NRG1.1 amino acids on a ZAR1-like functional N-terminal α-helix, were dispensible for their association (Fig. 6d). Together, these data argue for TNL effector recognition rendering bothNRG1 and EDS1-SAG101 competent to associate and confer pathogen resistance (Fig. 6e). Recently, the TIR domains of plant TNLs and certain truncated TIR forms were shown to exhibit an NADase activity (shown in Fig. 6e) that is necessary to induce plant *EDS1* dependent cell death [10, 11, 60]. Reported cryo-EM structures of effector-activated TNLs *Arabidopsis* RPP1 and *N. benthamiana* Roq1 reveal them to be tetrameric complexes with imposed TIR domain orientations creating an active NADase enzyme [8, 9]. Our findings suggest concerted actions between plant TNL NADase activity and immunity signalling via TNL-effector recognition induced EDS1-SAG101-NRG1 association. In our model (Fig. 6e), we envisage two paths for generating a signalling competent NRG1-EDS1-SAG101 complex . In path A, a TNL-derived NADase product binds to EDS1-SAG101, thereby enabling EP domain-dependent association with NRG1, perhaps triggering NRG1 oligomerization. In path B, the activated TNL receptor and/or NADase products cause an NRG1 nucleotide-dependent conformational change (independently of EDS1-SAG101) which promotes its association with EDS1-SAG101. The data presented here represent a significant advance by showing that pathogen-activated TNL receptors mediate downstream signalling via induced, specific interactions between RNLs and EDS1 family proteins.

Methods

Plant materials and growth conditions

Arabidopsis thaliana L. Heynh. (hereafter Arabidopsis) wild type, transgenic and mutant lines as well as *Nicotiana benthamiana* lines are listed in the Supplementary Table 1. For pathogen growth and cell death assays, Arabidopsis plants were grown under short day conditions (10 h light 22°C/14 h dark 20°C, light intensity of ~100 µmol m^{-2} sec^{-1}, 65% relative humidity) for 4-5 weeks. Crosses and seed propagation were conducted under speed breeding growth conditions: 22 h light 22°C/ 2 h dark 20°C, ~100 µmol m^{-2} sec^{-1}, 65% relative humidity. *N. benthamiana* plants were grown in a greenhouse under long day conditions for 5-6 weeks.

Cloning, site-directed mutagenesis and generation of complementation lines

Genomic Col-0 *SAG101* sequence (AT5G14930.2) including the coding and upstream (-992 bp) sequences were cloned into pENTR/D-TOPO (K240020, Thermo Fisher Scientific) and further LR-inserted (11791100, Thermo Fisher Scientific) into the expression vector pXCG-mYFP [61] resulting in pXCG pSAG101:SAG101-YFP. pXCSG p35S:NRG1.1-StrepII-3xHA as well as the pXCSG pADR1-L2:ADR1-L2-StrepII-3xHA constructs were described previously [26]. Constructs to express NRG1.1 mutant variants were prepared using the Golden gate MoIClo kit [62]. The genomic sequence of Col-0 *NRG1.1* (AT5G66900.1, from start ATG codon to the last codon position) was cloned into the level 0 plasmid pAGM1287, and the *NRG1.1* variants were generated following the QuikChange II Site-Directed mutagenesis (SDM) protocol (#200555, Agilent). Level 0 golden gate compatible construct for the genomic sequence of Col-0 *EDS1* (AT3G48090.1, from the first to the last codon) was synthesized and inserted into the pAM vector (GeneArt, Thermo Fisher Scientific). *EDS1*^{H476Y} and *EDS1*^{F419E} mutant constructs were generated via SDM. Primers for cloning and SDM are listed in Supplementary Table 2. To obtain level 1 expression constructs, level 0 constructs of *NRG1.1* mutants were combined with the cauliflower mosaic virus (CaMV) *35S* promoter (pICH51288), hemagglutinin tag (3xHA, pICSL50009), CaMV *35S* terminator (pICH41414) and the backbone pICH47732. Expression vectors for *EDS1* (p35S:EDS1^{H476Y}-3xFLAG, p35S:EDS1^{F419E}-3xFLAG) were cloned following the same strategy except the tag module was replaced by 3xFLAG (pICSL50007). The wild type p35S:EDS1-3xFLAG was prepared by LR-recombining pENTR/D-TOPO EDS1_noStop (genomic sequence of AT3G48090.1 from ATG to the last codon [30] with pAMPAT-3xFLAG [61]. p35S:PAD4-3xFLAG expression construct is a result of a LR reaction between pENTR/D-TOPO PAD4 [30] and pAMPAT-3xFLAG. p35S:3xFLAG-GUS was prepared by LR-recombining pJ2B-3xFLAG [61] with pENTR GUS (from LR clonase II kit, 11791020, Thermo Fisher Scientific). To prepare the *PAD4* expression construct for complementation, we PCR-amplified the *PAD4* locus (AT3G52430.1) from the upstream gene's stop codon (AT3G52420) up to the start codon of the downstream gene (AT3G52440) and placed it in a pDONR201 vector via PIPE-PCR [63]. Subsequently, N-terminal YFP with a linker peptide (Gly followed by 9x Ala) was introduced via PIPE-PCR as well. This construct was LR-recombined in a pAlligator2 destination vector [64]. Level 1 golden gate and gateway expression constructs were transformed via electroporation into *Rhizobium radiobacter* (hereafter *Agrobacterium tumefaciens* or Agrobacteria) GV3101 pMP90RK or pMP90 for transient expression in *N. benthamiana* and stable expression in Arabidopsis (Supplementary Table 3). We transformed pXCG pSAG101:SAG101-YFP and pAlligator2 pPAD4:YFP-Linker-PAD4 into Arabidopsis *pad4-1 sag101-3* mutant and selected homozygous complementation lines using BASTA resistance or the GFP seed coat fluorescence markers, respectively.

Pseudomonas growth and cell death assays in Arabidopsis

Pseudomonas syringae pv. *tomato* (*Pst*) DC3000 with the empty vector pVSP61, pVSP61 avrRps4 or pVSP61 avrRpt2 were syringe-infiltrated into Arabidopsis leaves at OD_{600}=0.0005 in 10 mM $MgCl_2$. Leaf discs were harvested at 0 dpi (four leaf discs as four technical replicates) and 3 dpi (12 leaf discs divided over four technical replicates). Biological replicates are experiments performed on different days with the same or different batches of plants. For cell death assays, *Pseudomonas fluorescens* effector tester strain *Pf*0-1 *avrRps4* [48] was resuspended in 10 mM $MgCl_2$ (OD_{600}=0.2) and syringe-infiltrated into leaves. Eight leaves per genotype were infiltrated for each biological replicate (experiments performed on different days with the same or different batches of plants). Conductivity of solution with the incubated leaf discs was measured at 6, 8, 10, and 24 hpi as described earlier [26]. Macroscopic cell death phenotype was recorded at 24 hpi. For cell death assays with *Pst avrRpt2*, bacteria were resuspended 10 mM $MgCl_2$ to OD_{600}=0.02 and electrolyte leakage was measured as described for *Pf*0-1 *avrRps4* triggered cell death. Means of three biological replicates (experiments performed on different days, four technical replicates each, n=12) were used to prepare heatmap with the pheatmap package in R. The statistical analysis included checking normality of residuals distribution (Shapiro-Wilcoxon at α=0.05 or visually with qq-plot) and homoscedasticity (Levene test at α=0.05). Difference in means was assessed via Tukey's HSD test (α=0.001, experiment taken as a factor in ANOVA).

Reconstitution of *Roq1* cell death and resistance assays in *N. benthamiana*

Roq1 cell death reconstitution assays were performed with the *Pf*0-1 *XopQ* [65] strain in *N. benthamiana* quadruple mutant *eds1a pad4 sag101a sag101b* (*Nb-epss*) [26]. *Agrobacteria* induced for one hour in Agromix (10 mM $MgCl_2$, 10 mM MES pH5.6, 150 µM acetosyringone) were firstly syringe-infiltrated at OD_{600}=0.2 into *Nb-epss* leaves. At 48hpi, *Pf*0-1 *XopQ* or *Pf*0-1 (empty vector) were infiltrated at OD_{600}=0.3 in the same leaf zone. At 24 hours after *Pf*0-1 *XopQ* infiltration, macroscopic cell death phenotype was recorded and four leaf discs (as four technical replicates) were taken for measuring electrolyte leakage at 6 h after collecting the leaf discs. *Xanthomonas campestris* pv. *vesicatoria* (*Xcv* 85-10; also *Xanthomonas euvesicatoria*) growth assays in *epss* in the presence of Agrobacteria to express proteins of interest were performed as described earlier [26].

Co-immunoprecipitation (co-IP) and immunoblotting analyses

In co-IP assays with proteins expressed in *N. benthamiana Roq1* reconstitution assays, five 10 mm leaf discs were collected to form a sample. Total protein from the plant material ground to fine powder was extracted in 2 ml of the extraction buffer (10% glycerol, 100 mM Tris-HCl pH7.5, 5 mM $MgCl_2$, 300 mM NaCl, 10 mM DTT, 0.5% NP-40, 2% PVPP, 1x Plant protease cocktail (11873580001, MilliporeSigma)). Lysates were centrifuged for 35 min at 4,500 x g and filtered through two layers of Miracloth (475855, MilliporeSigma). The 50 µl aliquots of the filtered supernatant were taken as input samples. Co-IP were conducted for 2 h with 12 µl α-HA affinity matrix (11815016001, MilliporeSigma) under constant rotation. Beads were collected by centrifugation at 4,000 x g for 1 min and washed four times in extraction buffer (without DTT and PVPP). All co-IP steps were conducted at 4°C. Beads and input samples were boiled at 95°C in 100 µl 2×Laemmli buffer for 10 min. Antibodies used for immunoblotting were α-GFP (11814460001, MilliporeSigma), α-HA (1:5000; c29f4, Cell Signalling), α-FLAG (1:5000; f1804, MilliporeSigma). Antibodies were used in dilution 1:5000 (TBST with 3% non-fat milk powder).

Immunoprecipitation (IP) of EDS1-YFP and TRB1-GFP from Arabidopsis complementation lines

Nuclei-enriched fractions were isolated from ~20 g of leaves of 4-5 week-old plants grown under short day conditions described above and vacuum-infiltrated with *Pst avrRps4* (OD_{600}=0.1, 10 mM $MgCl_2$ supplemented with 0.005% Silwet-L77). Samples were collected at 8-10 hours after the infiltration. After sample collection, all steps were conducted at 4°C or on ice. Extraction was performed mainly as in [66] with modifications. Leaves were chopped with a razor blade, all buffers contained 2xPlant Protease inhibitor cocktail (11873580001, MilliporeSigma). Separation was performed only on one Percoll gradient (80%-30%) followed by a final clean up though the 30% Percoll layer. Nuclei-enriched fractions were spun down for 10 min at 1,000 g to remove Percoll and hexylene glycol.

Nuclei-enriched fraction was gently resuspended in 1 ml of the sample buffer (20 mM Tris-HCl pH7.4, 2 mM MgCl2, 150 mM NaCl, 5% glycerol, 5 mM DTT, EDTA-free protease inhibitor (11873580001, MilliporeSigma)), centrifuged for 10 min at 1,000 g, and carefully resuspended again in 600 µl of the sample buffer. After incubation of washed nuclei at 37°C with 10 units of DNase I (89836, Thermo Fisher Scientific) and 20 µg of RNase A (EN0531, Thermo Fisher Scientific) under soft agitation for 15 min, samples were placed on ice for 10 min and sonicated for 6 cycles 15 sec "on" – 15 sec "off" using Bioruptor Plus (Diagenode). After that, samples were centrifuged for 15 min at 16,000 x g, and the supernatant was used as input for IP with GFP-trap A beads (per IP, 25 µl of slurry prewashed in 2 ml of the samples buffer, gta-100 (Proteintech)). Before IP, 25 µl of the supernatant is set aside as an input fraction for quality controls. Then, samples were supplemented with 10% Triton X-100 to the final concentration 0.1% and 0.5 M EDTA to the final concentration of 2 mM. After 2.5 hours of incubation with the sample in Protein Lobind tubes (0030108116 and 0030108132, Eppendorf), beads were washed four times in 300 µl 3 min each in the wash buffer (20 mM Tris-HCl pH7.4, 150 mM NaCl, 2 mM EDTA). Proteins were eluted in 2x35 µl 0.1% TFA and neutralized in 90 µl of Tris-Urea (4M urea 50mM Tris-HCl pH 8.5).

Gel filtration chromatography

Nuclear extracts (600 µl) from the *pEDS1:EDS1-YFP* complementation line were processed as for IP input in the subsection "Immunoprecipitation (IP) of EDS1-YFP and TRB1-GFP from respective Arabidopsis complementation lines". Obtained samples were fractionated on the column Superose 6 10/300 GL (50 kDa - 5 MDa range, GE Healthcare Life Sciences, Äkta FPLC) at the rate 0.5 ml/min in 20 mM Tris-HCl pH7.4 and 150 mM NaCl. The temperature was kept at 4°C. In total, 28 0.5 ml fractions per sample were collected, concentrated with StrataClean resin (400714, Agilent) and analyzed using Western blot method (α-GFP, 11814460001, MilliporeSigma) with the same total EDS1-YFP sample on each blot for the between-blot normalization. High-molecular weight marker was run prior each experiment (28403842, GE Healthcare Life Sciences).

IPs of YFP-PAD4 and SAG101-YFP from Arabidopsis complementation lines

Five-week-old Arabidopsis plants containing p35S:StrepII-3xHA-YFP (Col-0), pPAD4:YFP-PAD4 (*pad4-1 sag101-3* background) or pSAG101:SAG101-YFP (*pad4-1 sag101-3*) were vacuum infiltrated with *Pf*0-1 *avrRps4* bacteria (OD=0.2 in 10 mM $MgCl_2$ with 0.01% Silwet L-70). ~2 gram of rosette material was collected at 6 hpi, snap-frozen in liquid nitrogen and kept at -80°C until IP. On the day of IP, samples from were ground to fine powder in Precellys 15 ml tubes (P000946-LYSK0-A, Bertin Instruments). The protein extraction was performed in the 10 ml of the buffer composed of 20 mM PIPES-KOH pH7.0, 150 mM NaCl, 10 mM $MgCl_2$, 10% glycerol (v/v), 5 mM DTT, 1% Triton X-100, Plant Protease Inhibitor cocktail (11873580001, MilliporeSigma). The protein extraction was performed at 4°C for 20 min under constant end-to-end mixing (~60 rpm). After that, the samples were cleared by centrifuging 20 min at 4°C 3,000 x g. The supernatant was passed once through 0.2 µm filters (KC64.1, Roth)

to remove debris. Each sample (10 ml in 15 ml Falcon tubes) was incubated for 2.5 hours at 4°C under constant end-to-end mixing (~20 rpm) with equilibrated beads corresponding to 20 µl of GFP-trapA (gta100, Proteintech) slurry. After the incubation, beads were washed three times 5 min each with the wash buffer containing 20 mM Tris-HCl pH7.4, 150 mM NaCl, 0.01% Triton X-100, Plant Protease Inhibitor cocktail (11873580001, MilliporeSigma). Finally, to remove Triton X-100 traces, the beads were washed two additional times 1 min each in the buffer with 20 mM Tris-HCl pH7.4 and 150 mM NaCl.

Purification of NRG1.2 from the Arabidopsis complementation line

Arabidopsis Ws-2 *nrg1a nrg1b* complementation line from [19] was grown in short-day conditions for 5-6 weeks. *Pf*0-1 empty vector or *Pf*0-1 *avrRps4* were resuspended in the infiltration buffer (10 mM MES pH 5.7, 10 mM $MgCl_2$) at OD_{600}=0.3 and syringe-infiltrated into apoplastic space of rosette leaves. Approximately 2.5 g of tissue was harvested 4 hpi and flash frozen. Tissue was ground in liquid nitrogen before lysis in 100 mM HEPES (pH 7.5), 300 mM NaCl, 5 mM $MgCl_2$, 0.5% Nonidet P-40, 10 mM DTT, 10% glycerol, and cOmplete™ EDTA-free Protease Inhibitor Cocktail (11873580001, MilliporeSigma). Lysate was centrifuged at 4,000 *g* for 35 min at 4 °C and filtered through Miracloth to pellet and remove debris. Lysate was incubated with buffer equilibrated ANTI-FLAG® M2 Affinity Agarose beads (A2220, MilliporeSigma) for 45 min. Beads were washed before incubation with 3XFLAG® Peptide (F4799, Sigma-Aldrich) for 2 hrs. Eluate was collected for further analysis by immunoblot and mass spectroscopy.

Immunoblot analysis of NRG1.2-EDS1 interactions in Arabidopsis

Samples were heated in 4X SDS Sample Loading Buffer (10 mM DTT) at 65 °C for 5 min. Proteins were resolved on 4-20% SDS-PAGE (4561095, Bio-Rad) and dry transferred by Trans-Blot Turbo Transfer System to PVDF membrane (170427, Bio-Rad). Membranes were blocked in 5% milk (v/w) in TBST for 1 hr. For protein detection, HRP-conjugated anti-FLAG (A-8592, Sigma-Aldrich) was used at 1:30,000 (TBST, 5% milk powder [v/w]) and anti-EDS1 (AS13 2751, Agrisera) was used at 1:3000 (TBST, 3% milk powder [v/w]) and probed overnight at 4°C. Membranes were washed three times in TBS-T for 10 min. Secondary HRP-conjugated antibody (A0545, MilliporeSigma) was used at 1:10,000 (TBST, 5% milk powder [v/w]) at RT for 2 hrs. Membranes were washed three times in TBST for 10 min, and three times in TBS for 5 min. Detection of signal was performed with enhanced chemiluminescent horseradish peroxidase substrates SuperSignal™ West Pico PLUS (34580, Thermo Fischer Scientific) and Femto (34095, Thermo Fischer Scientific), and ImageQuant LAS 4000™ for protein band visualisation.

Arabidopsis NRG1.1 structure homology modelling

NRG1.1 (AT5G66900.1) was modelled on ZAR1 resistosome cryo-electron microscopy structure (PDB: 6j5tc1) using SWISS-MODEL. Visualization was performed in Pymol (Schrödinger, LLC).

673 **List of Supplemetary materials**

674 Supplementary Table 1. Plant genetic materials used in this study

675 Supplementary Table 2. Oligonucleotide sequences used in this study

676 Supplementary Table 3. *Agrobacteria* strains used in this study

677 Supplementary Text. Methods specific to LC-MS analyses presented in the study

678

679 **References**

680 1. Jones JDG, Vance RE, Dangl JL. Intracellular innate immune surveillance devices in
681 plants and animals. *Science (New York, NY)* **354**, aaf6395 (2016).
682
683 2. Tamborski J, Krasileva KV. Evolution of Plant NLRs: From Natural History to Precise
684 Modifications. *Annual review of plant biology* **71**, 355-378 (2020).
685
686 3. Wang J, Chai J. Molecular actions of NLR immune receptors in plants and animals.
687 *Science China Life Sciences* **63**, 1-14 (2020).
688
689 4. Monteiro F, Nishimura MT. Structural, Functional, and Genomic Diversity of Plant NLR
690 Proteins: An Evolved Resource for Rational Engineering of Plant Immunity. *Annual*
691 *Review of Phytopathology* **56**, 243-267 (2018).
692
693 5. Cui H, Tsuda K, Parker JE. Effector-triggered immunity: from pathogen perception to
694 robust defense. *Annual review of plant biology* **66**, 487-511 (2015).
695
696 6. Saur IML, Panstruga R, Schulze-Lefert P. NOD-like receptor-mediated plant immunity:
697 from structure to cell death. *Nature Reviews Immunology*, (2020).
698
699 7. Wang J*, et al.* Reconstitution and structure of a plant NLR resistosome conferring
700 immunity. *Science (New York, NY)* **364**, (2019).
701
702 8. Ma S*, et al.* Direct pathogen-induced assembly of an NLR immune receptor complex
703 to form a holoenzyme. *Science (New York, NY)* **370**, eabe3069 (2020).
704
705 9. Martin R*, et al.* Structure of the activated ROQ1 resistosome directly recognizing the
706 pathogen effector XopQ. *Science (New York, NY)* **370**, eabd9993 (2020).
707
708 10. Horsefield S*, et al.* NAD(+) cleavage activity by animal and plant TIR domains in cell
709 death pathways. *Science (New York, NY)* **365**, 793-799 (2019).
710
711 11. Wan L*, et al.* TIR domains of plant immune receptors are NAD(+)-cleaving enzymes
712 that promote cell death. *Science (New York, NY)* **365**, 799-803 (2019).
713
714 12. Saile SC*, et al.* Two unequally redundant "helper" immune receptor families mediate
715 Arabidopsis thaliana intracellular "sensor" immune receptor functions. *PLoS biology*
716 **18**, e3000783 (2020).
717
718 13. Mine A, Seyfferth C, Kracher B, Berens ML, Becker D, Tsuda K. The Defense
719 Phytohormone Signaling Network Enables Rapid, High-Amplitude Transcriptional
720 Reprogramming during Effector-Triggered Immunity. *The Plant cell* **30**, 1199-1219
721 (2018).
722

14. Bartsch M, *et al.* Salicylic acid-independent ENHANCED DISEASE SUSCEPTIBILITY1 signaling in Arabidopsis immunity and cell death is regulated by the monooxygenase FMO1 and the Nudix hydrolase NUDT7. *The Plant cell* **18**, 1038-1051 (2006).

15. Ngou BPM, Ahn H-K, Ding P, Jones JD. Mutual Potentiation of Plant Immunity by Cell-surface and Intracellular Receptors. 2020.2004.2010.034173 (2020).

16. Yuan M, *et al.* Pattern-recognition receptors are required for NLR-mediated plant immunity. *bioRxiv*, 2020.2004.2010.031294 (2020).

17. Jubic LM, Saile S, Furzer OJ, El Kasmi F, Dangl JL. Help wanted: helper NLRs and plant immune responses. *Current opinion in plant biology* **50**, 82-94 (2019).

18. Wu C-H, *et al.* NLR network mediates immunity to diverse plant pathogens. *Proceedings of the National Academy of Sciences* **114**, 8113 (2017).

19. Castel B, *et al.* Diverse NLR immune receptors activate defence via the RPW8-NLR NRG1. *The New phytologist* **222**, 966-980 (2019).

20. Peart JR, Mestre P, Lu R, Malcuit I, Baulcombe DC. NRG1, a CC-NB-LRR Protein, together with N, a TIR-NB-LRR Protein, Mediates Resistance against Tobacco Mosaic Virus. *Current Biology* **15**, 968-973 (2005).

21. Collier SM, Hamel L-P, Moffett P. Cell Death Mediated by the N-Terminal Domains of a Unique and Highly Conserved Class of NB-LRR Protein. *Molecular Plant-Microbe Interactions®* **24**, 918-931 (2011).

22. Bonardi V, Tang S, Stallmann A, Roberts M, Cherkis K, Dangl JL. Expanded functions for a family of plant intracellular immune receptors beyond specific recognition of pathogen effectors. *Proceedings of the National Academy of Sciences of the United States of America* **108**, 16463-16468 (2011).

23. Daskalov A, *et al.* Identification of a novel cell death-inducing domain reveals that fungal amyloid-controlled programmed cell death is related to necroptosis. *Proceedings of the National Academy of Sciences of the United States of America* **113**, 2720-2725 (2016).

24. Mahdi LK, *et al.* Discovery of a Family of Mixed Lineage Kinase Domain-like Proteins in Plants and Their Role in Innate Immune Signaling. *Cell host & microbe* **28**, 813-824 (2020).

25. Wu Z, *et al.* Differential regulation of TNL-mediated immune signaling by redundant helper CNLs. *The New phytologist* **222**, 938-953 (2019).

26. Lapin D, *et al.* A Coevolved EDS1-SAG101-NRG1 Module Mediates Cell Death Signaling by TIR-Domain Immune Receptors. *The Plant cell* **31**, 2430-2455 (2019).

27. Wiermer M, Feys BJ, Parker JE. Plant immunity: the EDS1 regulatory node. *Current opinion in plant biology* **8**, 383-389 (2005).

28. Lapin D, Bhandari DD, Parker JE. Origins and Immunity Networking Functions of EDS1 Family Proteins. *Annual Review of Phytopathology* **58**, 253-276 (2020).

29. Gantner J, Ordon J, Kretschmer C, Guerois R, Stuttmann J. An EDS1-SAG101 Complex Is Essential for TNL-Mediated Immunity in Nicotiana benthamiana. *The Plant cell* **31**, 2456-2474 (2019).

30. Wagner S*, et al.* Structural basis for signaling by exclusive EDS1 heteromeric complexes with SAG101 or PAD4 in plant innate immunity. *Cell host & microbe* **14**, 619-630 (2013).

31. Rietz S*, et al.* Different roles of Enhanced Disease Susceptibility1 (EDS1) bound to and dissociated from Phytoalexin Deficient4 (PAD4) in Arabidopsis immunity. *The New phytologist* **191**, 107-119 (2011).

32. Bhandari DD*, et al.* An EDS1 heterodimer signalling surface enforces timely reprogramming of immunity genes in Arabidopsis. *Nature communications* **10**, 772 (2019).

33. Cui H, Gobbato E, Kracher B, Qiu J, Bautor J, Parker JE. A core function of EDS1 with PAD4 is to protect the salicylic acid defense sector in Arabidopsis immunity. *The New phytologist* **213**, 1802-1817 (2017).

34. Tanaka S, Han X, Kahmann R. Microbial effectors target multiple steps in the salicylic acid production and signaling pathway. *Frontiers in Plant Science* **6**, 349 (2015).

35. Qi T*, et al.* NRG1 functions downstream of EDS1 to regulate TIR-NLR-mediated plant immunity in Nicotiana benthamiana. *Proceedings of the National Academy of Sciences of the United States of America* **115**, E10979-e10987 (2018).

36. Saucet SB, Ma Y, Sarris PF, Furzer OJ, Sohn KH, Jones JDG. Two linked pairs of Arabidopsis TNL resistance genes independently confer recognition of bacterial effector AvrRps4. *Nature communications* **6**, 6338 (2015).

37. Venugopal SC*, et al.* Enhanced disease susceptibility 1 and salicylic acid act redundantly to regulate resistance gene-mediated signaling. *PLoS genetics* **5**, e1000545 (2009).

38. Tsuda K, Sato M, Stoddard T, Glazebrook J, Katagiri F. Network properties of robust immunity in plants. *PLoS genetics* **5**, e1000772 (2009).

39. Coll NS, Smidler A, Puigvert M, Popa C, Valls M, Dangl JL. The plant metacaspase AtMC1 in pathogen-triggered programmed cell death and aging: functional linkage with autophagy. *Cell Death & Differentiation* **21**, 1399-1408 (2014).

40. Coll NS*, et al.* Arabidopsis type I metacaspases control cell death. *Science (New York, NY)* **330**, 1393-1397 (2010).

41. Roberts M, Tang S, Stallmann A, Dangl JL, Bonardi V. Genetic requirements for signaling from an autoactive plant NB-LRR intracellular innate immune receptor. *PLoS genetics* **9**, e1003465 (2013).

42. Rustérucci C, Aviv DH, Holt BF, 3rd, Dangl JL, Parker JE. The disease resistance signaling components EDS1 and PAD4 are essential regulators of the cell death pathway controlled by LSD1 in Arabidopsis. *The Plant cell* **13**, 2211-2224 (2001).

43. García AV*, et al.* Balanced nuclear and cytoplasmic activities of EDS1 are required for a complete plant innate immune response. *PLoS pathogens* **6**, e1000970 (2010).

44. Feys BJ, Moisan LJ, Newman MA, Parker JE. Direct interaction between the Arabidopsis disease resistance signaling proteins, EDS1 and PAD4. *EMBO J* **20**, 5400-5411 (2001).

45. Feys BJ*, et al.* Arabidopsis SENESCENCE-ASSOCIATED GENE101 stabilizes and signals within an ENHANCED DISEASE SUSCEPTIBILITY1 complex in plant innate immunity. *The Plant cell* **17**, 2601-2613 (2005).

46. Voss M, Toelzer C, Bhandari DD, Parker JE, Niefind K. Arabidopsis immunity regulator EDS1 in a PAD4/SAG101-unbound form is a monomer with an inherently inactive conformation. *Journal of structural biology* **208**, 107390 (2019).

47. Zhou Y, Hartwig B, James GV, Schneeberger K, Turck F. Complementary Activities of TELOMERE REPEAT BINDING Proteins and Polycomb Group Complexes in Transcriptional Regulation of Target Genes. *The Plant cell* **28**, 87-101 (2016).

48. Thomas WJ, Thireault CA, Kimbrel JA, Chang JH. Recombineering and stable integration of the Pseudomonas syringae pv. syringae 61 hrp/hrc cluster into the genome of the soil bacterium Pseudomonas fluorescens Pf0-1. *The Plant journal : for cell and molecular biology* **60**, 919-928 (2009).

49. Sohn KH*, et al.* The Nuclear Immune Receptor RPS4 Is Required for RRS1SLH1-Dependent Constitutive Defense Activation in Arabidopsis thaliana. *PLoS genetics* **10**, e1004655 (2014).

50. Wei H-L, Zhang W, Collmer A. Modular Study of the Type III Effector Repertoire in Pseudomonas syringae pv. tomato DC3000 Reveals a Matrix of Effector Interplay in Pathogenesis. *Cell Reports* **23**, 1630-1638 (2018).

51. Schultink A, Qi T, Lee A, Steinbrenner AD, Staskawicz B. Roq1 mediates recognition of the Xanthomonas and Pseudomonas effector proteins XopQ and HopQ1. *The Plant Journal* **92**, 787-795 (2017).

52. Tameling WI*, et al.* The tomato R gene products I-2 and MI-1 are functional ATP binding proteins with ATPase activity. *The Plant cell* **14**, 2929-2939 (2002).

53. Williams SJ*, et al.* An autoactive mutant of the M flax rust resistance protein has a preference for binding ATP, whereas wild-type M protein binds ADP. *Molecular plant-microbe interactions : MPMI* **24**, 897-906 (2011).

54. El Kasmi F*, et al.* Signaling from the plasma-membrane localized plant immune receptor RPM1 requires self-association of the full-length protein. *Proceedings of the National Academy of Sciences of the United States of America* **114**, E7385-e7394 (2017).

55. Mestre P, Baulcombe DC. Elicitor-Mediated Oligomerization of the Tobacco N Disease Resistance Protein. *The Plant cell* **18**, 491-501 (2006).

56. Burdett H*, et al.* The Plant "Resistosome": Structural Insights into Immune Signaling. *Cell host & microbe* **26**, 193-201 (2019).

57. Jirage D*, et al.* Arabidopsis thaliana PAD4 encodes a lipase-like gene that is important for salicylic acid signaling. *Proceedings of the National Academy of Sciences of the United States of America* **96**, 13583-13588 (1999).

58. Morel J-B, Dangl JL. The hypersensitive response and the induction of cell death in plants. *Cell Death & Differentiation* **4**, 671-683 (1997).

59. Straus MR, Rietz S, Ver Loren van Themaat E, Bartsch M, Parker JE. Salicylic acid antagonism of EDS1-driven cell death is important for immune and oxidative stress responses in Arabidopsis. *The Plant journal : for cell and molecular biology* **62**, 628-640 (2010).

60. Duxbury Z*, et al.* Induced proximity of a TIR signaling domain on a plant-mammalian NLR chimera activates defense in plants. *Proceedings of the National Academy of Sciences* **117**, 18832 (2020).

61. Witte CP, Noël LD, Gielbert J, Parker JE, Romeis T. Rapid one-step protein purification from plant material using the eight-amino acid StrepII epitope. *Plant molecular biology* **55**, 135-147 (2004).

62. Engler C*, et al.* A golden gate modular cloning toolbox for plants. *ACS synthetic biology* **3**, 839-843 (2014).

63. Klock HE, Lesley SA. The Polymerase Incomplete Primer Extension (PIPE) method applied to high-throughput cloning and site-directed mutagenesis. *Methods in molecular biology (Clifton, NJ)* **498**, 91-103 (2009).

64. Bensmihen S, To A, Lambert G, Kroj T, Giraudat J, Parcy F. Analysis of an activated ABI5 allele using a new selection method for transgenic Arabidopsis seeds. *FEBS letters* **561**, 127-131 (2004).

65. Gantner J*, et al.* Peripheral infrastructure vectors and an extended set of plant parts for the Modular Cloning system. *PloS one* **13**, e0197185 (2018).

66. Folta KM, Kaufman LS. Isolation of Arabidopsis nuclei and measurement of gene transcription rates using nuclear run-on assays. *Nature protocols* **1**, 3094-3100 (2006).

Acknowledgements. We thank Franziska Turck (MPIPZ) for providing seeds of the TRB1-GFP complementation line and Deepak D. Bhandari (at MPIPZ, since 2019 at Michigan State University) for help with gel filtration chromatography. This work was supported by the Max-Planck Society and Deutsche Forschungsgemeinschaft (DFG) grants SFB 680 (J.E.P., D.L.) and SFB-1403–414786233 (J.E.P., X.S.); DFG-ANR Trilateral ("RADAR" grant to J.E.P. and J.A.D.) and a Chinese Scholarship Council doctoral fellowship to X.S.

Author contributions. X.S., D.L., J.M.F., K.K., S.C.S., A.H., P.D., F.L.H.M, I.F., H.N. contributed immunoprecipitation and LC-MS data; X.S., D.L., J.M.F., H.N., I.F., J.D.G.J., J.E.P. designed experiments and analysed data; X.S., J.A.D., J.B., J.R., S.B. generated and characterized genetic material; X.S. and J.R. performed cell death and pathogen infection assays; X.S., D.L., J.M.F., J.D.G.J., J.E.P. wrote the manuscript with contributions from all authors.

Competing interests. All authors declare no competing interests.

Materials & Correspondence. Correspondence and material requests should be addressed to J Jane E. Parker (parker@mpipz.mpg.de) and Jonathan D.G. Jones (jonathan.jones@TSL.ac.uk)

Figure Legends

Fig. 1. Distinct *PAD4/ADR1*s and *SAG101/NRG1*s-dependent mechanisms in *Arabidopsis* TNL immunity. (a) Overview of mutants used in (b) and (c). Group I comprises mutants disabled in *SAG101* and/or *NRG1*s: *sag101, nrg1.1 nrg1.2* (*n2*) and *sag101 n2*. Group II has mutants in *PAD4* and/or *ADR1*s: *pad4*, *adr1 adr1-L1 adr1-L2* (*a3*) and *pad4 a3*. Group III is composed of cross-branch combinatorial mutants *a3 n2*, *sag101 a3*, *pad4 n2*, *pad4 sag101*, *sag101 pad4 a3*, *sag101 pad4 n2*, *eds1 pad4 sag101*. **(b)** Growth of *Pseudomonas syringae pv. tomato* DC3000 (*Pst*) *avrRps4* in leaves of *Arabidopsis* Col-0 (Col) and indicated mutants at 3 days post inoculation (dpi) via syringe infiltration (OD_{600}=0.0005). Bacterial loads are shown as $\log_{10}$ colony-forming units (CFU) per cm^2. Experiments were performed three times independently with four replicates each (Tukey's HSD, α=0.001, n=12). **(c)** Growth of *Pst avrRps4*, *Pst avrRpt2* or *Pst* (empty vector, EV) in indicated *Arabidopsis* lines at 3 dpi via syringe infiltration (OD_{600}=0.0005). Heatmap represents mean $\log_{10}$-transformed CFU values from three independent experiments, each with four replicates (n=12). Statistical significance codes are assigned based on Tukey's HSD (α=0.001, n=12). The jitter plot in (b) shows individual data points used to calculate means on the heatmap for *Pst avrRps4* infection. *sag101 a3* and *pad4 n2* phenocopy *pad4 sag101* and *a3 n2*, indicating that *SAG101* does not form functional signalling modules with *ADR1s*, and *NRG1s* with *PAD4*.

Fig. 2. *PAD4* with *ADR1s* promotion of $TNL^{RRS1\text{-}RPS4}$ cell death is exposed in lines with non-functional *ICS1* and *SAG101-NRG1*s. (a) A heatmap representation of *Pst avrRps4*, *Pst avrRpt2* or *Pst* (empty vector, EV) growth at 3 dpi in leaves of indicated genotypes (syringe infiltration OD_{600}=0.0005). The significance codes are based on the Tukey's HSD test (α=0.001, n=12-16). Data points were combined from three (*Pst avrRps4*, *Pst avrRpt2*) or four (*Pst*) independent experiments, each with four replicates. **(b)** A heatmap of quantitative cell death assays conducted on leaves of indicated genotypes after infiltration utilizing the *Pseudomonas fluorescens* 0-1 effector tester strain (hereafter *Pf*0-1) delivering *avrRps4* (OD_{600}=0.2). Cell death was measured by electrolyte leakage from bacteria-infiltrated leaf discs at 6, 8, 10 and 24 hpi. Data are displayed as means from four experiments, each with four replicates (n=16). Statistical significance codes for the difference in means are based on Tukey's HSD test (α=0.001). In mutants marked in red, the *PAD4-ADR1s* cell death branch operates in $TNL^{RRS1\text{-}RPS4}$ immunity when *SAG101-NRG1s* and *ICS1* pathways are not functional. **(c)** Visual cell death symptoms at 24 hpi *Pf*0-1 *avrRps4* infiltrating into leaf halves of indicated genotypes as in (b). The ratio beneath each leaf indicates number of leaves with visible tissue collapse from all infiltrated leaves in two independent experiments. White arrows

mark cell death visible as tissue collapse in a manner dependent on *SAG101-NRG1s*. Red arrows mark cell death in lines without functional *SAG101-NRG1s* and *ICS1*.

Fig. 3. Early effector-dependent NRG1 association with EDS1 and SAG101 in *Arabidopsis* TNL$^{RRS1\text{-}RPS4}$ triggered ETI. **(a)** Heat map of normalized abundance values (LFQ, $\log_2$ scaled) for proteins detected in liquid chromatography mass-spectrometry (LC-MS) analyses after α-GFP immunoprecipitation (IP) of PAD4-YFP or SAG101-YFP from total leaf extracts of respective complementation lines *pPAD4:YFP-PAD4* and *pSAG101:SAG101-YFP* (both Col *pad4 sag101* background) after infiltration with *Pf*0-1 *avrRps4* (6 hpi, OD_{600}=0.2). ADR1s are specifically enriched in PAD4-YFP IP samples, whereas NRG1s are more abundant in the SAG101-YFP IP samples. Samples were collected from four independent experiments. All protein values shown $|\Delta\log_2 LFQ|\geq 1$, $p\leq 0.05$ (relative to YFP-SH IP). Asterisks indicate detection in three of four replicates. Grey indicates not detected or detected in < 3 of 4 replicates. **(b)** Heat map of LFQ values for proteins detected in LC-MS analyses after IP of EDS1-YFP and TRB1-GFP from nuclei-enriched extracts of corresponding *Arabidopsis* complementation lines [43, 47] infiltrated with *Pst avrRps4* (8 hpi, OD_{600}=0.1). NRG1.1 and NRG1.2 are specifically enriched in EDS1-YFP samples. Samples were collected from four independent experiments. All shown protein $|\Delta\log_2 LFQ|\geq 1$, $p\leq 0.05$ (relative to TRB1-GFP IP). Grey means the protein is not detected or detected in <3 of 4 replicates.**(c)** α-GFP probed immunoblots of nuclei-enriched extracts from leaves of the *Arabidopsis pEDS1:EDS1-YFP* complementation line (Col *eds1-2* background) infiltrated with *Pst avrRps4* (OD_{600}=0.1, 8 hpi). Extracts were resolved using native gel filtration. Arrows below protein markers indicate position of the corresponding peak. Numbers refer to column fractions. EDS1 forms stable ~100-600 kDa complexes. The experiment was repeated three times with similar results. **(d)** LC-MS analysis of eluates after α-FLAG IP of total leaf extracts from *Arabidopsis* Ws-2 *n2 pNRG1.2:NRG1.2-HF* complementation line [19] infiltrated with *Pf*0-1 EV or *Pf*0-1 *avrRps4* (4 hpi, OD_{600}=0.3). Peptides corresponding to EDS1 and SAG101 were observed in eluates only after *Pf*0-1-mediated delivery of avrRps4. This result was observed in two independent experiments. **(e)** Immunoblot analysis of eluates from (d). Asterisk indicates a nonspecific band on the α-EDS1 blot for input samples. The analysis was performed on total leaf extracts and was repeated four times with similar results. Association of EDS1 with NRG1.2-HF was observed only after *Pf*0-1-mediated delivery of avrRps4. Ponceau S staining shows equal protein loading in input samples on the blot.

Fig. 4. TNL^{Roq1} effector recognition-dependent *Arabidopsis* NRG1 association with EDS1 and SAG101 in *N. benthamiana.* (a) Sample collection scheme for experiments in (b) and (c). Roq1 dependent cell death is restored in the *Nb eds1 pad4 sag101a sag101b* (*Nb-epss*) signalling deficient mutant by expressing *Arabidopsis* EDS1, SAG101 and NRG1.1 via Agrobacteria infiltration 48 h before XopQ effector delivery. *Pf*0-1 *XopQ* is syringe-infiltrated (OD_{600}=0.3) to deliver the effector in a time-resolved manner and study TNL signalling events up to 24 hpi. **(b)** Macroscopic symptoms and quantification of XopQ-triggered cell death at 24 hpi after infiltrating *Pf*0-1 *XopQ* in leaves of *Nb-epss* expressing *Arabidopsis* EDS1-FLAG, SAG101-FLAG, NRG1.1-3xHA-StrepII (NRG1.1-SH) or ADR1-L2-3xHA-StrepII (ADR1-L2-SH). *Pf*0-1 served as a "no-ETI" control. Cell death was quantified in electrolyte leakage assays 6 h after harvesting leaf discs (24 hpi with *Pf*0-1 *XopQ*). The experiment was performed three times independently, each with four technical replicates (leaf discs) (Tukey's HSD, α=0.001, n=12). Transiently expressed *Arabidopsis* EDS1, SAG101 and NRG1.1 proteins are functional in *Pf*0-1 *XopQ* triggered (*Roq1*) cell death. **(c)** Coimmunoprecipitation assay followed by Western blotting to test for XopQ-triggered associations between *Arabidopsis* NRG1.1-SH and FLAG-tagged EDS1 or SAG101 in *Nb-epss* according to the infiltration scheme in (a). NRG1.1-SH or ADR1-SH were enriched using α-HA agarose beads, and presence of FLAG-tagged EDS1, SAG101 or GUS was tested by probing blots with α-FLAG antibodies. IP assays were repeated three times independently with similar results. NRG1.1 association with EDS1 and SAG101 requires Roq1/XopQ ETI activation.

Fig. 5. Effector-dependent NRG1-EDS1-SAG101 association requires a functional EDS1 EP domain. (a) Representation of the *Arabidopsis* EDS1 (green) - SAG101 (purple) heterodimer crystal structure (PDB: 4NFU) with highlighted EP-domain cavity surfaces that are essential for TNL triggered cell death (Lapin et al., 2019). An α-helix of the SAG101 EP-domain (blue) and residues F419 (magenta) and H476 (orange) in the EDS1 EP-domain are shown as ribbon and spheres, respectively. **(b,c)** Roq1/XopQ dependent cell death (b) and bacterial resistance (c) in leaves of *Nb-epss* transiently expressing of C-terminally FLAG-tagged EDS1 wildtype and mutant variants with SAG101-FLAG and NRG1.1-SH or ADR1-L2-SH. Cell death was triggered by infiltrating *Pf*0-1 *XopQ* at 48 h after Agrobacteria infiltration to express the *Arabidopsis* proteins; photos of leaf discs for the electrolyte leakage assays were taken at 24 h. Roq1 resistance to *Xanthomonas campestris pv. vesicatoria* (*Xcv*) strain 85-10 expressing XopQ. F419E and H476Y mutations in the *Arabidopsis* EDS1 EP-domain abrogated cell death and resistance, as shown in [26] using different plasmid backbones and tags. Experiments were performed three times independently, each with four replicates (leaf discs) (Tukey's HSD, α=0.001, n=12). **(d)** IP followed by Western blot analysis to test

dependency of associations between *Arabidopsis* EDS1-SAG101 and NRG1.1 in *Nb-epss* on a functional EDS1 EP- domain cavity. Leaves of *Nb-epss* were infiltrated with Agrobacteria to express FLAG-tagged EDS1 or its variants EDS1^{F419E} and EDS1^{H476Y}, SAG101-FLAG and NRG1.1-SH or PAD4-FLAG, with ADR1-L2-SH and GUS-FLAG as negative controls. At 2 dpi, *Pf*0-1 *XopQ* (OD_{600}=0.3) was infiltrated, and the triggered samples were collected at 10 hpi. Following IP with α-HA agarose beads, input and and IP fractions were probed with α-HA and α-FLAG antibodies. Roq1/XopQ dependent association of NRG1.1-SH with EDS1-FLAG and SAG101-FLAG was abolished in samples with mutated EDS1 EP-domain variants. Similar results were obtained in three independent experiments.

Fig. 6. Association between *Arabidopsis* NRG1.1, EDS1 and SAG101 requires an intact NRG1.1 P-loop. (a) A structure homology model of *Arabidopsis* NRG1.1 based on the ZAR1 resistosome (PDB: 6J5T, chains G-O). NRG1.1 amino acids E14 and E27 (red sticks) and L21 and K22 (blue sticks) are predicted to align with functionally defined residues E11, E18, F9, L10 and L14 in the N-terminal ZAR1 α1-helix. The modelled NRG1.1 P-loop motif (G199 K200 T201) is shown as cyan sticks. *Pf*0-1 *XopQ*-triggered cell death **(b)** and bacterial (*Xcv*) growth restriction **(c)** in *Nb-epss* expressing *Arabidopsis* NRG1.1-SH wildtype, NRG1.1$^{E14A/E27A}$, NRG1.1$^{L21A/K22A}$ and NRG1.1$^{G199A/K200A/T201A}$ variants together with EDS1-FLAG and SAG101-FLAG. *Arabidopsis* proteins were expressed via Agrobacteria-mediated transient expression assays 2 d before *Pf*0-1 *XopQ* (OD_{600}=0.3) or simultaneously with *Xcv* (OD_{600}=0.0005) infiltration. An intact NRG1.1 predicted N-terminal α-helix and P-loop are required for NRG1.1 function in reconstituted *Roq1* ETI cell death and pathogen resistance. Experiments were performed three times independently, each with four technical replicates (leaf discs) (Tukey's HSD, α=0.001, n=12). **(d)** IP and Western blot analyses testing associations of *Arabidopsis* NRG1.1 mutant variants with EDS1 and SAG101 in *Nb-epss* after triggering *Roq1* signalling by *Pf*0-1 *XopQ* infiltration (OD_{600}=0.3; 10 hpi). *Arabidopsis* EDS1-FLAG, SAG101-FLAG with NRG1.1-SH, and using GUS-FLAG and *Arabidopsis* ADR1-L2-SH as negative controls, were expressed using Agrobacteria 2 d prior to *Pf*0-1 *XopQ* infiltration. After α-HA IP, the indicated fractions were analyzed with α-HA and α-FLAG antibodies by Western blotting. An NRG1.1 intact P-loop but not N-terminal amino acids are essential for Roq1/XopQ-dependent NRG1.1 association with the EDS1-SAG101 dimer. The experiment was repeated three times independently with similar results. **(e)** Model of molecular events leading to generation of an *Arabidopsis* EDS1-SAG101-NRG1 signalling complex that is essential for TNL receptor activated defence. NRG1-EDS1-SAG101 association is dependent on TNL-effector activation and requires an intact EDS1-SAG101 heterodimer EP domain cavity (purple circle) and NRG1 nucleotide binding domain P-loop motif. In two depicted

scenarios, an effector-induced TNL oligomer with NADase activity leads to activation (asterisks) of EDS1-SAG101 via the EP domain cavity ('Path A', asterisk inside the purple circle) or NRG1 ('Path B'). These paths are not mutually exclusive. EDS1-SAG101-NRG1 assembly precedes and is necessary for TNL triggered cell death and resistance involving a predicted NRG1 N-terminal HeLo domain α-helix.

Supplementary Figure 1

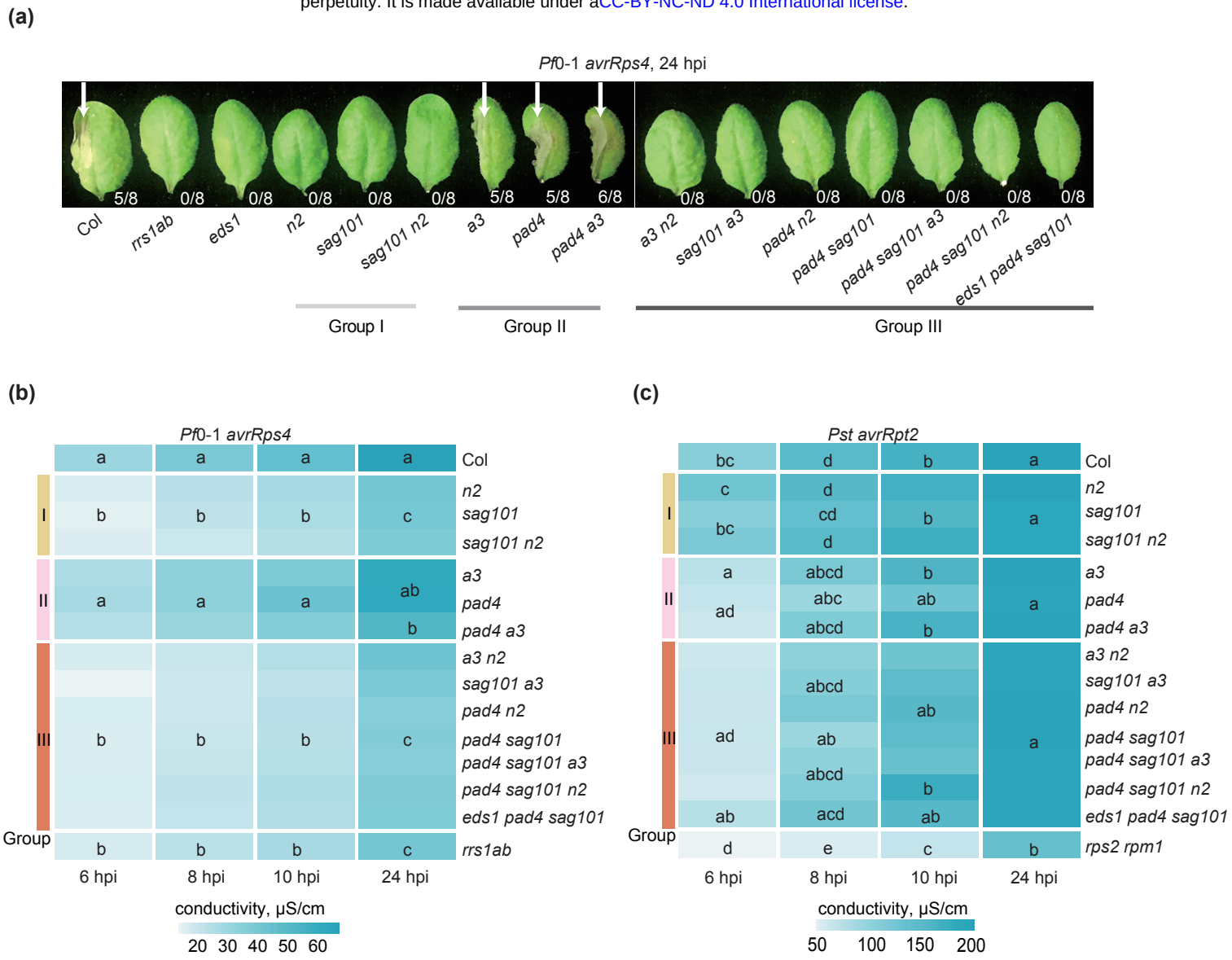

Supplementary Figure 1. No evidence for the cross-use of components between the *PAD4-ADR1*s and *SAG101-NRG1*s branches in *Arabidopsis* NLR cell death. Related to Fig. 1. **(a)** Macroscopic symptoms of TNL$^{RRS1-RPS4}$ cell death triggered by *Pf*0-1 *avrRps4* in Col-0 (Col), *rrs1a rrs1b* (*rrs1ab*), and mutants with mutated *SAG101* and/or *NRG1*s (group I), *PAD4* and/or *ADR1*s (group II) or their cross-branch combinations (group III). White arrow indicates cell death visible as tissue collapse at 24 hours post bacteria infiltration (hpi). Numbers indicate number of leaves with visible tissue collapse from the total number of infiltrated leaves from four plants in one experiment. The experiment was repeated three times with similar results. **(b, c)** A heatmap of electrolyte leakage to quantify cell death at 6, 8, 10 and 24 hpi with *Pf*0-1 *avrRps4* (OD_{600}=0.2) (b) or *Pst avrRpt2* (OD_{600}=0.02) for indicated genotypes as in (a) and the *rpm1 rps2* mutant. Data are displayed as mean conductivity from three independent experiments with four technical replicates each. Statistical analysis used posthoc Tukey's HSD test (α=0.001, n=12). *PAD4* and *SAG101* do not form signalling branches with *NRG1*s and *ADR1*s, respectively, to promote receptor NLR-dependent (RRS1-RPS4 and RPS2) cell death.

Supplementary Figure 2

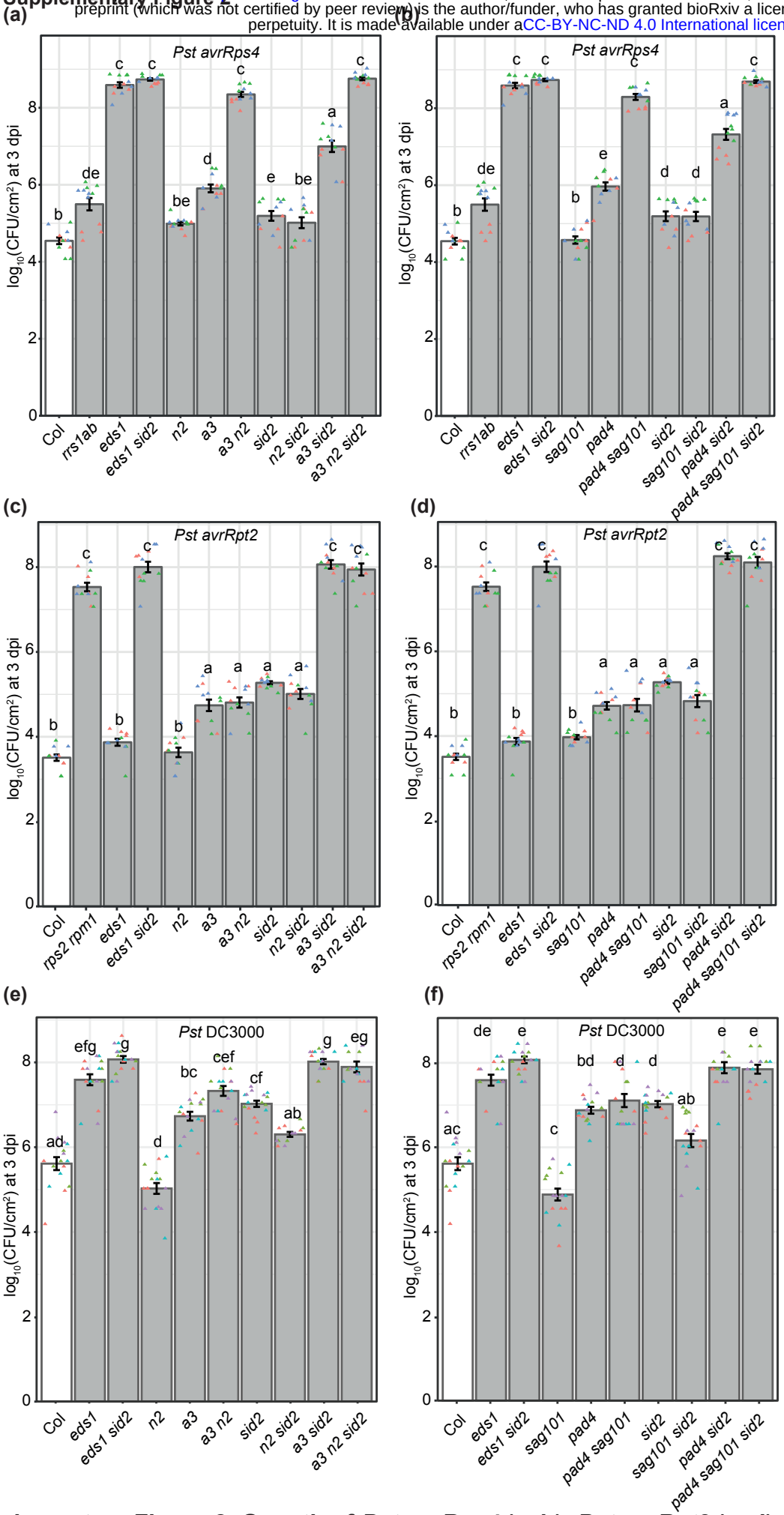

Supplementary Figure 2. Growth of *Pst avrRps4* (a, b), *Pst avrRpt2* (c, d) and *Pst* (empty vector, (e, f)) in mutants defective in *ICS1/SID2* and *PAD4-ADR1*s or *SAG101-NRG1*s branches. Related to Fig. 2a. Bacterial loads are expressed as colony forming units (CFU) per cm^2 at 3 dpi on a log_{10} scale. Bacteria were syringe-infiltrated (OD_{600}=0.0005). The experiments were performed three times independently with four technical replicates (leaf discs) each (Tukey's HSD, α=0.001, n=12).

Supplementary Figure 3

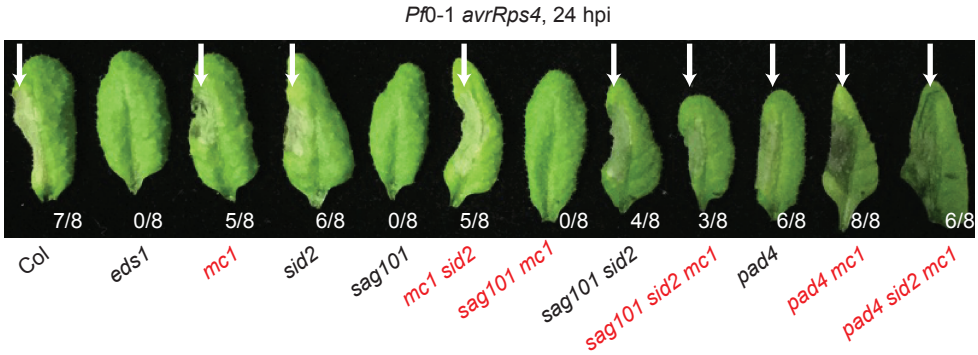

Supplementary Figure 3. *Metacaspase 1* (*MC1*) is dispensable for the TNL$^{RRS1\text{-}RPS4}$ cell death involving *SAG101-NRG1*s and *PAD4-ADR1*s. Macroscopic symptoms of cell death triggered by *Pf*0-1 *avrRps4* (OD_{600}=0.2) in Col-0 (Col) single (*eds1*, *sag101*, *pad4*, *sid2*, *mc1*) and indicated combinatorial mutants. White arrows point to collapsed leaf areas at 24 hpi. Genotypes in red contain the *mc1* mutation. Eight leaves from four plants were syringe-infiltrated with *Pf*0-1 *avrRps4*, and the number of collapsed leaves was counted at 24 hpi. The experiment was repeated three times with similar results.

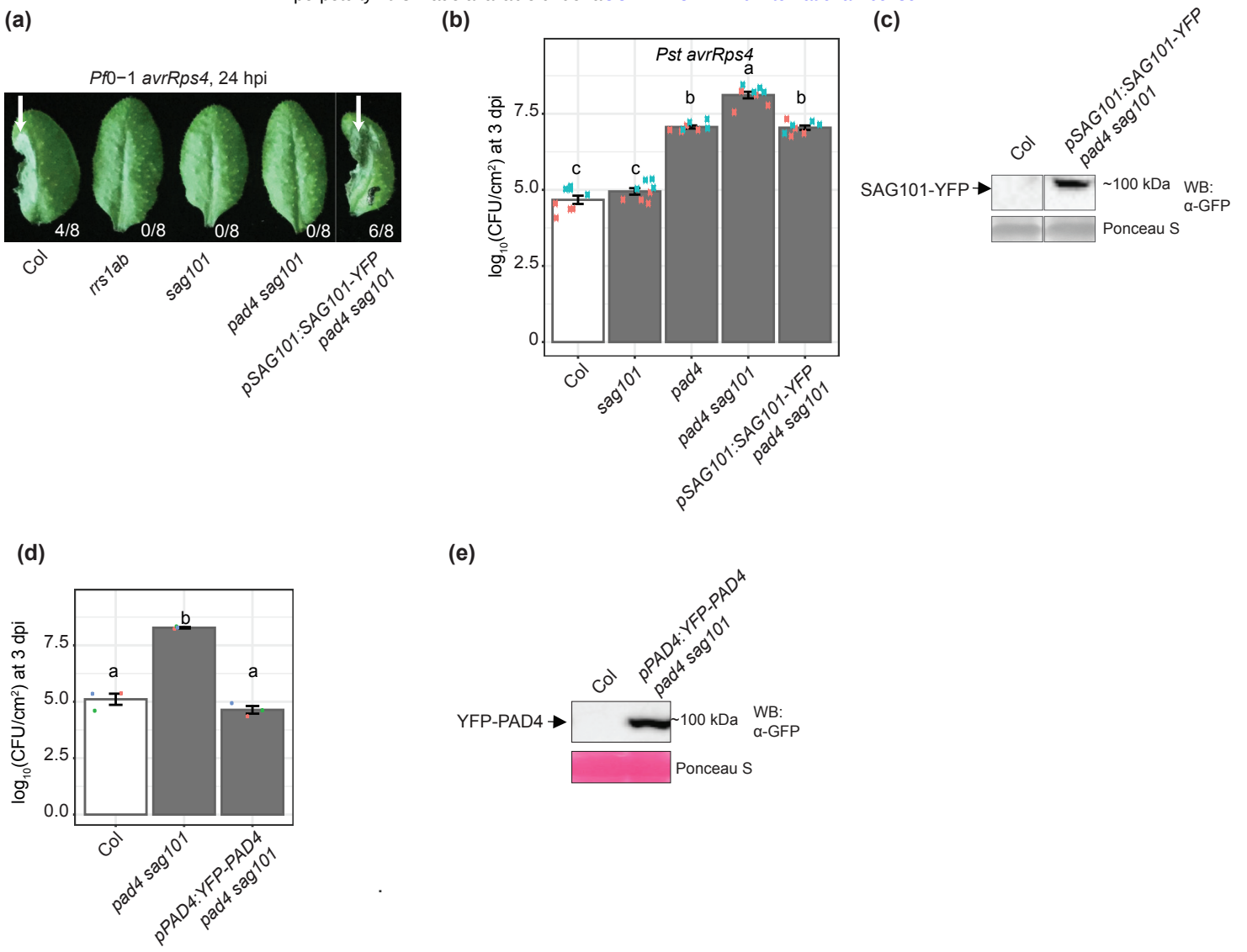

Supplementary Figure 4. Characterization of the complementation lines carrying *pSAG101:SAG101-YFP* and *pPAD4:YFP-PAD4* in the Col-0 *pad4 sag101* background. (a, b) Complementation in the *pSAG101:SAG101-YFP* (*pad4 sag101*) T3 homozygous line was assessed using RRS1-RPS4 cell death (a) and bacterial resistance (b) assays with Col-0 (Col), *rrs1a rrs1b* (*rrs1ab*), *sag101* and *pad4 sag101* as controls. (a) Cell death was examined visually at 24 hpi of *Pf*0-1 *avrRps4*. Numbers refer to the number of leaves showing tissue collapse vs. all infiltrated leaves. The experiment was repeated three times with similar results. (b) *Pst avrRps4* titers ($\log_{10}$ of CFU/cm2) were determined at 3 dpi after bacteria syringe-infiltration (OD_{600}=0.0005). The experiment was performed twice with four technical replicates each (Tukey's HSD, α=0.001, n=8). Both *SAG101*-dependent RPS4-RRS1 cell death and resistance were recovered by the *pSAG101:SAG101-YFP* construct transformed into the signalling-defective *pad4 sag101* mutant. **(c)** Western blot analysis SAG101-YFP steady-state levels in the transgenic line in (a, b) using α-GFP antibodies. Bands were cropped from same blot. The experiment was performed twice. The SAG101-YFP fusion protein produced a band of the indicated expected size. **(d)** *Pst avrRps4* titers in *pPAD4:YFP-PAD4 pad4 sag101* T3 homozygous line at 3 dpi (OD_{600}=0.0005; syringe infiltration) (three independent experiments, one technical replicate from each, Tukey's HSD, α=0.001, n=3). (e) Immunoblot analysis of PAD4-YFP steady-state levels in the transgenic line in (d) using α-GFP antibody. The Western blotting detection was repeated two times with similar results.

Supplementary Figure 5

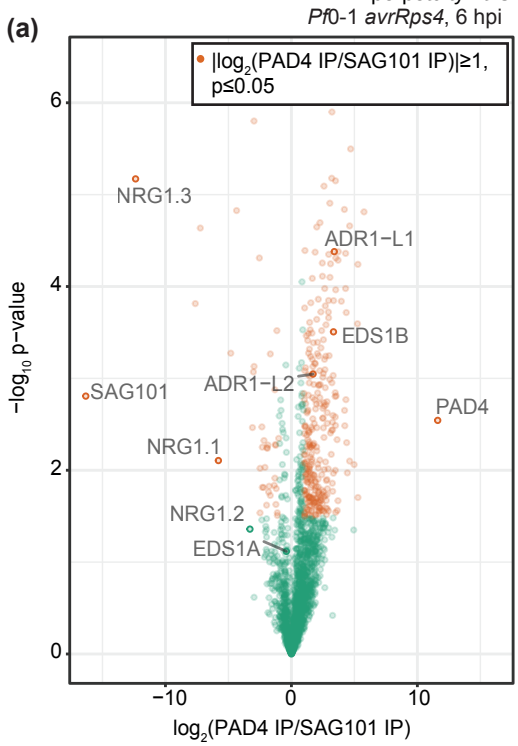

Supplementary Figure 5. Selective enrichment of RNLs with SAG101 and PAD4 in *Arabidopsis* leaves upon activation of TNL$^{RRS1\text{-}RPS4}$. (a) Volcano plot of normalized abundances (LFQ, $\log_2$ scale) for proteins copurified with YFP-PAD4 and SAG101-YFP from total leaf extracts of the respective complementation lines *pPAD4:YFP-PAD4* and *pSAG101:SAG101-YFP* (both Col-0 *pad4 sag101* background) infiltrated with *Pf*0-1 *avrRps4* (6 hpi, OD_{600}=0.2). Proteins enriched in PAD4-YFP vs. SAG101-YFP IPs are shown in orange (($|\log_2$(PAD4 IP/SAG101 IP)|≥1, permutation p≤0.05). Missing values were imputed. NRG1.1, NRG1.2 and NRG1.3 are enriched in the SAG101-YFP samples, while ADR1 and ADR1-L1 were detected only on PAD4-YFP samples. The IP-MS analysis was performed on samples collected in four independent experiments.

Supplementary Figure 6

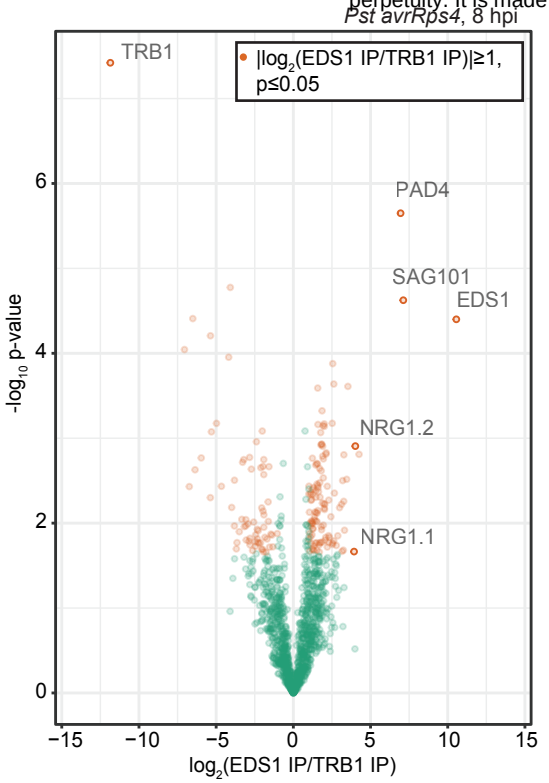

Supplementary Figure 6. NRG1 proteins specifically co-purify with EDS1 in *Arabidopsis* leaves upon activation of TNL-RRS1-RPS4. Volcano plot of normalized abundances (LFQ, $\log_2$ scale) of proteins detected in mass-spectrometry (MS) analyses after immunoprecipitation (IP) of EDS1-YFP and TRB1-GFP from nuclear extracts of corresponding *Arabidopsis* complementation lines infiltrated with *Pst avrRps4* (8 hpi, OD_{600}=0.1). In orange are proteins enriched in EDS1-YFP vs. TRB1-GFP samples ($|\log_2$(EDS1-YFP/TRB1-GFP)|≥1, permutation p≤0.05; missing values imputed). Samples for the MS analysis were collected in four independent experiments. NRG1.1 and NRG1.2 are specifically enriched in EDS1-YFP samples.

Supplementary Figure 1. No evidence for the cross-use of components between the *PAD4-ADR1*s and *SAG101-NRG1*s branches in *Arabidopsis* NLR cell death. Related to Fig. 1. **(a)** Macroscopic symptoms of TNL (RRS1-RPS4) cell death triggered by *Pf*0-1 *avrRps4* in Col-0 (Col), *rrs1a rrs1b* (*rrs1ab*), and mutants with mutated *SAG101* and/or *NRG1*s (group I), *PAD4* and/or *ADR1*s (group II) or their cross-branch combinations (group III). White arrow indicates cell death visible as tissue collapse at 24 hours post bacteria infiltration (hpi). Numbers indicate number of leaves with visible tissue collapse from the total number of infiltrated leaves from four plants in one experiment. The experiment was repeated three times with similar results. **(b, c)** A heatmap of electrolyte leakage to quantify cell death at 6, 8, 10 and 24 hpi with *Pf*0-1 *avrRps4* (OD_{600}=0.2) (b) or *Pst avrRpt2* (OD_{600}=0.02) for indicated genotypes as in (a) and the *rpm1 rps2* mutant. Data are displayed as mean conductivity from three independent experiments with four technical replicates each. Statistical analysis used posthoc Tukey's HSD test (α=0.001, n=12). *PAD4* and *SAG101* do not form signaling branches with *NRG1*s and *ADR1*s, respectively, to promote receptor NLR-dependent (RRS1-RPS4 and RPS2) cell death.

Supplementary Figure 2. Growth of *Pst avrRps4* (a, b), *Pst avrRpt2* (c, d) and *Pst* (empty vector, (e, f)) in mutants defective in *ICS1/SID2* and *PAD4-ADR1*s or *SAG101-NRG1*s branches. Related to Fig. 2a. Bacterial loads are expressed as colony forming units (CFU) per cm^2 at 3 dpi on a log_{10} scale. Bacteria were syringe-infiltrated (OD_{600}=0.0005). The experiments were performed three times independently with four technical replicates (leaf discs) each (Tukey's HSD, α=0.001, n=12).

Supplementary Figure 3. *Metacaspase 1* (*MC1*) is dispensable for the TNL RRS1-RPS4 cell death involving *SAG101-NRG1*s and *PAD4-ADR1*s. Macroscopic symptoms of cell death triggered by *Pf*0-1 *avrRps4* (OD_{600}=0.2) in Col-0 (Col) single (*eds1*, *sag101*, *pad4*, *sid2*, *mc1*) and indicated combinatorial mutants. White arrows point to collapsed leaf areas at 24 hpi. Genotypes in red contain the *mc1* mutation. Eight leaves from four plants were syringe-infiltrated with *Pf*0-1 *avrRps4*, and the number of collapsed leaves was counted at 24 hpi. The experiment was repeated three times with similar results.

Supplementary Figure 4. Characterization of the complementation lines carrying *pSAG101:SAG101-YFP* and *pPAD4:YFP-PAD4* in the Col-0 *pad4 sag101* background. (a, b) Complementation in the *pSAG101:SAG101-YFP* (*pad4 sag101*) T3 homozygous line was assessed using RPS4-RRS1 cell death (a) and bacterial resistance (b) assays with Col-0 (Col), *rrs1a rrs1b* (*rrs1ab*), *sag101* and *pad4 sag101* as controls. (a) Cell death was examined visually at 24 hpi of *Pf*0-1 *avrRps4*. Numbers refer to the number of leaves showing tissue collapse vs. all

infiltrated leaves. The experiment was repeated three times with similar results. (b) *Pst avrRps4* titers (log_{10} of CFU/cm^2) were determined at 3 dpi after bacteria syringe-infiltration (OD_{600}=0.0005). The experiment was performed twice with four technical replicates each (Tukey's HSD, α=0.001, n=8). Both SAG101-dependent RPS4-RRS1 cell death and resistance were recovered by the *pSAG101:SAG101-YFP* construct transformed into the signaling-defective *pad4 sag101* mutant. **(c)** Western blot analysis SAG101-YFP steady-state levels in the transgenic line in (a, b) using α-GFP antibodies. Bands were cropped from same blot. The experiment was performed twice. The SAG101-YFP fusion protein produced a band of the indicated expected size. **(d)** *Pst avrRps4* titers in *pPAD4:YFP-PAD4 pad4 sag101* T3 homozygous line at 3 dpi (OD_{600}=0.0005; syringe infiltration) (three independent experiments, one technical replicate from each, Tukey's HSD, α=0.001, n=3). **(e)** Immunoblot analysis of PAD4-YFP steady-state levels in the transgenic line in (d) using α-GFP antibody. The detection was repeated two times with similar results.

Supplementary Figure 5. Selective enrichment of RNLs with SAG101 and PAD4 in Arabidopsis leaves upon activation of TNL$^{RRS1\text{-}RPS4}$. Volcano plot of normalized abundances (LFQ, log_2 scale) for proteins copurified with PAD4-YFP and SAG101-YFP from total leaf extracts of the respective complementation lines *pPAD4:YFP-PAD4* and *pSAG101:SAG101-YFP* (both Col-0 *pad4 sag101* background) infiltrated with *Pf*0-1 *avrRps4* (6 hpi, OD_{600}=0.2). Proteins enriched in PAD4-YFP vs. SAG101-YFP IPs are shown in orange (($|log_2$(YFP-PAD4/SAG101-YFP)$|\geq 1$, permutation $p \leq 0.05$). Missing values were imputed. NRG1.1, NRG1.2 and NRG1.3 are enriched in the SAG101-YFP samples, while ADR1 and ADR1-L1 were detected only on PAD4-YFP samples. The IP-MS analysis was performed on samples collected in four independent experiments.

Supplementary Figure 6. NRG1 proteins specifically co-purify with EDS1 in *Arabidopsis* leaves upon activation of TNL$^{RRS1\text{-}RPS4}$. Volcano plot of normalized abundances (LFQ, log_2 scale) of proteins detected in mass-spectrometry (MS) analyses after immunoprecipitation (IP) of EDS1-YFP and TRB1-GFP from nuclear extracts of corresponding *Arabidopsis* complementation lines infiltrated with *Pst avrRps4* (8 hpi, OD_{600}=0.1). In orange are proteins enriched in EDS1-YFP vs. TRB1-GFP samples ($|log_2$(EDS1-YFP/TRB1-GFP)$|\geq 1$, permutation $p \leq 0.05$; missing values imputed). Samples for the MS analysis were collected in four independent experiments. NRG1.1 and NRG1.2 are specifically enriched in EDS1-YFP samples.

Supplementary Figure 7. Multiple sequence alignments of selected helper RPW8 domain NLRs (RNLs), helper CNLs (NRC), receptor CNLs and TNLs over the P-loop motif sequences. The P-

loop is indicated with red line. Multiple sequence alignments were built (Clustal Omega) and visualised with the msa package in R. Accession numbers of NLRs in the alignment: NRG1.1 – AT5G66900.1, NRG1.2 – AT5G66910.1, *Lus*NRG1 - Lus10022464, *Nb*NRG1 - Niben101Scf02118g00018.1, *At*ADR1-L2 - AT5G04720.1, *Sl*ADR1 - Solyc04g079420.3.1, *Nb*ADR1 - Niben101Scf02422g02015.1, *Sl*NRC4 - Solyc04g007070.3.1, *Sl*NRC3 - XP_004238948.1, *At*ZAR1 - AT3G50950.2, N - Q40392, Roq1 - ATD14363.1, RPP4 - F4JNA9, RPS4 - Q9XGM3, RPM1 - Q39214, Rx - Q9XGF5.

Supplementary Text

Methods (continued)

Preparation of peptides for LC-MS/MS analysis in IP experiments with EDS1-YFP and TRB1-GFP complementation lines

Immunoprecipitated proteins in Tris-Urea were reduced with dithiothreitol, alkylated with chloroacetamide, and digested with trypsin (1:100) o/n. Samples were desalted using stage tips with C18 Empore disk membranes (3 M) [1].

Preparation of peptides for LC-MS/MS analysis in IP experiments with YFP-PAD4 and SAG101-YFP complementation lines

Proteins (from GFP-trapA enrichment) were submitted to an on-bead digestion. In brief, dry beads were re-dissolved in 25 µL digestion buffer 1 (50 mM Tris, pH 7.5, 2M urea, 1mM DTT, 5 ng/µL trypsin) and incubated for 30 min at 30°C in a Thermomixer with 400 rpm. Next, beads were pelleted, and the supernatant was transferred to a fresh tube. Digestion buffer 2 (50 mM Tris, pH 7.5, 2M urea, 5 mM CAA) was added to the beads, after mixing the beads were pelleted, the supernatant was collected and combined with the previous one. The combined supernatants were then incubated o/n at 32 °C in a Thermomixer with 400 rpm; samples were protected from light during incubation. The digestion was stopped by adding 1 µL TFA and desalted with C18 Empore disk membranes according to the StageTip protocol [1].

Label-free LC-MS/MS data acquisition and data processing for IP experiments with EDS1-YFP, YFP-PAD4, SAG101-YFP and TRB1-GFP

Dried peptides were re-dissolved in 2% ACN, 0.1% TFA (10 µL) for analysis and measured without dilution. Samples were analyzed using an EASY-nLC 1200 (Thermo Fisher Scientific) coupled to a Q Exactive Plus mass spectrometer (Thermo Fisher Scientific). Peptides were separated on 16 cm frit-less silica emitters (New Objective, 0.75 µm inner diameter), packed in-house with reversed-phase ReproSil-Pur C18 AQ 1.9 µm resin (Dr. Maisch). Peptides were loaded on the column and eluted for 115 min using a segmented linear gradient of 5% to 95% solvent B (0 min: 5%B; 0-5 min -> 5%B; 5-65 min -> 20%B; 65-90 min ->35%B; 90-100 min -> 55%; 100-105 min ->95%, 105-115 min ->95%) (solvent A 0% ACN, 0.1% FA; solvent B 80% ACN, 0.1%FA) at a flow rate of 300 nL/min. Mass spectra were acquired in data-dependent acquisition mode with a TOP15 method. MS spectra were acquired in the Orbitrap analyzer with a mass range of 300–1750 m/z at a resolution of 70,000 FWHM and a target value of 3×106 ions. Precursors were selected with an isolation window of 1.3 m/z. HCD fragmentation was performed at a normalized collision energy of 25. MS/MS spectra were acquired with a target value of 105 ions at a resolution of 17,500 FWHM, a maximum injection time (max.) of 55 ms and a fixed first mass of m/z 100. Peptides with a charge of +1, greater than 6, or with unassigned charge state were excluded from fragmentation for MS2, dynamic exclusion for 30s prevented repeated selection of precursors.

Raw data were processed using MaxQuant software (version 1.6.3.4, http://www.maxquant.org/) [2] with label-free quantification (LFQ) and iBAQ enabled [2, 3]. MS/MS spectra were searched by the Andromeda search engine against a combined database containing the sequences from A. thaliana (TAIR10_pep_20101214; ftp://ftp.arabidopsis.org/home/tair/Proteins/TAIR10_protein_lists/) and sequences of 248 common contaminant proteins and decoy sequences. Trypsin specificity was required and a maximum of two missed cleavages allowed. Minimal peptide length was set to seven amino acids. Carbamidomethylation of cysteine residues was set as fixed, oxidation of methionine and protein N-terminal acetylation as variable modifications. Peptide-spectrum-matches and proteins were retained if they were below a false discovery rate of 1%. Statistical analysis of

the MaxLFQ values was carried out using Perseus (version 1.5.8.5, http://www.maxquant.org/). Quantified proteins were filtered for reverse hits and hits "identified by site" and MaxLFQ values were $\log_2$ transformed. After grouping samples by condition only those proteins were retained for the subsequent analysis that had three valid values in one of the conditions. Two-sample t-tests were performed using a permutation-based FDR of 5%. Alternatively, quantified proteins were grouped by condition and only those hits were retained that had 4 valid values in one of the conditions. Missing values were imputed from a normal distribution (1.8 downshift, separately for each column). Volcano plots were generated in Perseus using an FDR of 5% and an S0=1. The Perseus output was exported and further processed using Excel.

LC-MS/MS analysis of NRG1.2-copurified proteins

Samples were resolved by SDS-PAGE with RunBlueTM 4-20% TEO-Tricine (BCG42012) and stained with InstantBlue® Coomassie Protein Stain (ab119211). Bands were excised from gel with sterile blade and stored at – 20 °C if not submitted fresh. LC-MS and data processing was carried out as previously described [4]. Data was analysed as total spectrum counts in Scaffold Viewer (Proteome Software) and filtered for a protein threshold probability > 99%, peptide threshold probability > 95%, and a minimum of two peptides identified.

Supplementary Table 1. Plant genetic materials used in this study

Denoted name	Full name	Description, reference
eds1	Col-0/L*er eds1-2* (multiple backcrosses to Col-0)	[5]
sag101	Col-0 *sag101-3* (GABI-Kat 476E10)	[6]
pad4	Col-0 *pad4-1*	[7]
pad4 sag101	*pad4-1 sag101-3*	[6]
eds1 pad4 sag101	*eds1-2 pad4-1 sag101-3*	[8]
sid2	*sid2-1*	[9]
eds1 sid2	*eds1-2 sid2-1*	[6]
pad4 sid2	*pad4-1 sid2-1*	[6]
sag101 sid2	*sag101-3 sid2-1*	This study, cross between *eds1-2 sag101-3 pad4-1* and *sid2-1*
pad4 sag101 sid2	*pad4-1 sag101-3 sid2-1*	This study, cross between *eds1-2 sag101-3 pad4-1* and *sid2-1*
n2	*nrg1.1 nrg1.2*	[10]
a3	*adr1 adr1-L1 adr1-L2*	[11]
n2 a3	*nrg1.1 nrg1.2 adr1 adr1-L1 adr1-L2*	[10]
n2 sid2	*nrg1.1_nrg1.2_sid2-1*	This study, cross between *n2 a3* and *sid2*
a3 sid2	*adr1 adr1-L1 adr1-L2 sid2-1*	
a3 n2 sid2	*nrg1.1 nrg1.2 adr1 adr1-L1 adr1-L2 sid2-1*	
sag101 n2	*nrg1.1 nrg1.2 sag101-3*	This study, cross between *n2 a3* and *eds1 sag101 pad4*
pad4 n2	*nrg1.1 nrg1.2 pad4-1*	
sag101 a3	*adr1 adr1-L1 adr1-L2 sag101-3*	
pad4 a3	*adr1 adr1LI1 adr1-L2 pad4-1*	
sag101 pad4 a3	*adr1 adr1-L1 adr1-L2 sag101-3 pad4-1*	
sag101 pad4 n2	*nrg1.1 nrg1.2 sag101-3 pad4-1*	
mc1	*mc1-1* (GABI-Kat 096A10)	[12]
mc1 sid2	*mc1 sid2-1*	This study, cross between *mc1* and *pad4 sag101 sid2*
sag101 mc1	*sag101-3 mc*	This study, cross between *mc1* and *pad4 sag101 sid2*
sag101 sid2 mc1	*sag101-3 sid2-1 mc1*	This study, cross between *mc1* and *pad4 sag101 sid2*
pad4 mc1	*pad4-1 mc1*	This study, cross between *mc1* and *pad4 sag101 sid2*
pad4 sid2 mc1	*pad4-1 sid2-1 mc1*	This study, cross between *mc1* and *pad4 sag101 sid2*
pEDS1:EDS1-YFP	pXCG *pEDS1:EDS1-YFP*, Col-0/L*er eds1-2*	(García et al., 2010), for MS analysis
p35S:TRB1-GFP	pAM-PAT p35S:TRB1-GFP Col-0 *trb1-1*	[13]
p35:StrepII-3xHA-YFP	pAM-PAT StrepII-3xHA-YFP Col-0	[10]
pSAG101:SAG101-YFP	pXCG pSAG101:SAG101-YFP, *pad4-1 sag101-3*	This study
pPAD4:PAD4-YFP	pAlligator2 pPAD4:YFP-PAD4, *pad4-1 sag101-3*	This study
pNRG1.2:NRG1.2-HF	pNRG1.2:NRG1.2-6xHis-3xFLAG, Ws-2 *nrg1a nrg1b*	[14]
Nb-epss	*N. benthamiana eds1a pad4 sag101a sag101b*	(Lapin et al., 2019)
N. bethamiana wild type	*N.benthamiana* (MPIPZ stock)	(Lapin et al., 2019)

Supplementary Table 3. Agrobacteria strains used in this study

Strain name	Full name	Strain
dDL276	p35S:NRG1.1-StrepII-3xHA	GV3101 pMP90RK [10]
dXS323	p35S:NRG1.1$^{E14A/E27A}$-3xHA	GV3101 pMP90RK
dXS318	p35S:NRG1.1$^{L21A/K22A}$-3xHA	GV3101 pMP90RK
dXS320	p35S:NRG1.1^{G199AK200AT201A}-3xHA	GV3101 pMP90RK
dJDQ367	p35S:EDS1-3xFLAG	GV3101 pMP90RK
dXS334	p35S:EDS1^{H476Y}-3xFLAG	GV3101 pMP90RK
dXS338	p35S:EDS1^{F419E}-3xFLAG	GV3101 pMP90RK
MW30	pEDS1:EDS1-YFP	GV3101 pMP90RK
dXS298	p35S:SAG101-3xFLAG	GV3101 pMP90RK
dDL336	pADR1-L2:ADR1_L2- StrepII-3xHA	GV3101 pMP90RK [10]
dXS264	p35S:3xFLAG-GUS	GV3101 pMP90RK
CLR071	p35S:PAD4-3xFLAG	GV3101 pMP90RK

References for Supplementary materials

1. Rappsilber J, Ishihama Y, Mann M. Stop and go extraction tips for matrix-assisted laser desorption/ionization, nanoelectrospray, and LC/MS sample pretreatment in proteomics. *Analytical chemistry* **75**, 663-670 (2003).

2. Cox J, Mann M. MaxQuant enables high peptide identification rates, individualized p.p.b.-range mass accuracies and proteome-wide protein quantification. *Nature biotechnology* **26**, 1367-1372 (2008).

3. Tyanova S, Temu T, Cox J. The MaxQuant computational platform for mass spectrometry-based shotgun proteomics. *Nature protocols* **11**, 2301-2319 (2016).

4. Bender KW*, et al.* Autophosphorylation-based Calcium (Ca(2+)) Sensitivity Priming and Ca(2+)/Calmodulin Inhibition of Arabidopsis thaliana Ca(2+)-dependent Protein Kinase 28 (CPK28). *The Journal of biological chemistry* **292**, 3988-4002 (2017).

5. Bartsch M*, et al.* Salicylic acid-independent ENHANCED DISEASE SUSCEPTIBILITY1 signaling in Arabidopsis immunity and cell death is regulated by the monooxygenase FMO1 and the Nudix hydrolase NUDT7. *The Plant cell* **18**, 1038-1051 (2006).

6. Cui H, Gobbato E, Kracher B, Qiu J, Bautor J, Parker JE. A core function of EDS1 with PAD4 is to protect the salicylic acid defense sector in Arabidopsis immunity. *The New phytologist* **213**, 1802-1817 (2017).

7. Jirage D*, et al.* Arabidopsis thaliana PAD4 encodes a lipase-like gene that is important for salicylic acid signaling. *Proceedings of the National Academy of Sciences of the United States of America* **96**, 13583-13588 (1999).

8. Wagner S*, et al.* Structural basis for signaling by exclusive EDS1 heteromeric complexes with SAG101 or PAD4 in plant innate immunity. *Cell host & microbe* **14**, 619-630 (2013).

9. Wildermuth MC, Dewdney J, Wu G, Ausubel FM. Isochorismate synthase is required to synthesize salicylic acid for plant defence. *Nature* **414**, 562-565 (2001).

10. Lapin D*, et al.* A Coevolved EDS1-SAG101-NRG1 Module Mediates Cell Death Signaling by TIR-Domain Immune Receptors. *The Plant cell* **31**, 2430-2455 (2019).

11. Bonardi V, Tang S, Stallmann A, Roberts M, Cherkis K, Dangl JL. Expanded functions for a family of plant intracellular immune receptors beyond specific recognition of pathogen effectors. *Proceedings of the National Academy of Sciences of the United States of America* **108**, 16463-16468 (2011).

12. Coll NS, Smidler A, Puigvert M, Popa C, Valls M, Dangl JL. The plant metacaspase AtMC1 in pathogen-triggered programmed cell death and aging: functional linkage with autophagy. *Cell Death & Differentiation* **21**, 1399-1408 (2014).

13. Zhou Y, Hartwig B, James GV, Schneeberger K, Turck F. Complementary Activities of TELOMERE REPEAT BINDING Proteins and Polycomb Group Complexes in Transcriptional Regulation of Target Genes. *The Plant cell* **28**, 87-101 (2016).

14. Castel B*, et al.* Diverse NLR immune receptors activate defence via the RPW8-NLR NRG1. *The New phytologist* **222**, 966-980 (2019).